
Doctoral Dissertations

Student Theses and Dissertations

Summer 1983

Theoretical studies of water on substrates

Sergio M. Terrazas

Follow this and additional works at: https://scholarsmine.mst.edu/doctoral_dissertations

 Part of the [Physics Commons](#)

Department: **Physics**

Recommended Citation

Terrazas, Sergio M., "Theoretical studies of water on substrates" (1983). *Doctoral Dissertations*. 1034.
https://scholarsmine.mst.edu/doctoral_dissertations/1034

This thesis is brought to you by Scholars' Mine, a service of the Missouri S&T Library and Learning Resources. This work is protected by U. S. Copyright Law. Unauthorized use including reproduction for redistribution requires the permission of the copyright holder. For more information, please contact scholarsmine@mst.edu.

THEORETICAL STUDIES OF WATER ON SUBSTRATES

BY

SERGIO M. TERRAZAS, 1952 -

A DISSERTATION

Presented to the Faculty of the Graduate School of the

UNIVERSITY OF MISSOURI - ROLLA

In Partial Fulfillment of the Requirements for the Degree

DOCTOR OF PHILOSOPHY

in

PHYSICS

July 1983

Barbara R. Hale
Advisor

Gerald P. Alldredge

[Signature]

Jerry L. Pescher

Harry A. Brown

ABSTRACT

Model interaction potentials for H_2O on a basal β -silver iodide substrate containing two types of defects, a potassium impurity and a four atomic layer ledge, are used to calculate optimal binding energy contours for the adsorbed H_2O molecule. (J. Phys. Chem. 84, 1473(1980)). The model substrate with the potassium impurity appears to increase the optimal binding energy at the preferred adsorption sites to 23 kcal/mol -- a value approximately 40 % larger than the maximal binding energy sites on the defect-free model silver-exposed basal plane of AgI. The impurity also distorts the hexagonal symmetry of the preferred adsorption sites, drawing them towards the impurity. The four-layer ledge produces sites parallel to the ledge with optimal binding energy equal to 23 kcal/mol -- compared to 20 (16) kcal/mol for maximal binding energy sites on the prism (iodine-exposed basal) face of the defect-free model AgI substrate. In a second study a formalism is presented for estimating the critical cluster size, n^* , and steady state nucleation rate, J , for adsorbed monolayer formation. The latter is combined with a Metropolis Monte Carlo technique and applied to water clusters on a featureless Lennard-Jones substrate with average H_2O -substrate binding energy and short range forces parameters comparable to the model iodine-exposed basal AgI substrate. At 265 °K, the values $1 < n^* < 2$ and, $J \sim 10^{24} \text{cm}^{-2} \text{sec}^{-1}$ are predicted at water saturation. A comparison with results for water adsorbed on the model iodine-exposed basal AgI substrate (J. Chem. Phys. 78, 420(1983)) indicates that on both substrates a water monolayer forms rapidly and with approximately the same nucleation rate. The present results give an order of magnitude larger value of J for the smooth substrate and hence imply that the latter forms a monolayer at lower vapor pressures than the model AgI.

ACKNOWLEDGEMENTS

I want to express my deepest sense of gratitude to my advisor, Dr. Barbara Hale, for her guidance and her patience that went well above and beyond the call of duty. Without her encouragement in difficult times I would never have reached this point. I also want to thank Dr. Jerry Peacher, Dr. Gerald Alldredge, Dr. Josef Podzimek, and Dr. Harry Brown for serving in my committee and for their useful comments and constructive criticism. My special appreciation goes to Harry Brown, the friend and teacher who made my stay at UMR much more pleasant. I thank Dr. Richard Ward for his continuous help with all aspects of the computer calculations and for having developed the basic computer program for the Monte Carlo method.

I am indebted to the Physics department of UMR for the financial support during part of my stay and to its chairman, Dr. John Park, who is always concerned about the well-being of the students. I want to acknowledge the financial support of the National Council of Science and Technology (Mexico). This material is based upon work supported by the National Science Foundation under Grant ATM80-15790.

Finally, I want to give the credit due to my family for sharing with me all these years of the often difficult life of a student.

TABLE OF CONTENTS

ABSTRACT.	ii
ACKNOWLEDGEMENTS.	iii
TABLE OF CONTENTS	iv
LIST OF ILLUSTRATIONS	vi
LIST OF TABLES.	xi
I. INTRODUCTION	1
A. MOTIVATION FOR THIS WORK.	1
B. SUMMARY OF PREVIOUS STUDIES OF H ₂ O ON AgI	4
C. DISCUSSION OF THE PRESENT WORK.	7
II. THE BASAL PLANES OF AgI WITH DEFECTS	10
A. THE POTASSIUM IMPURITY.	10
1. The model substrate and the interaction potentials.	10
2. Calculations and results.	14
B. THE FOUR LAYER LEDGE.	19
III. THE BINDING ENERGY AS A FUNCTION OF EFFECTIVE CHARGE	25
A. MAXIMAL BINDING ENERGY AS A FUNCTION OF CHARGE	25
B. COMPARISON OF AVERAGE BINDING ENERGIES WITH EXPERIMENT.	32

IV.	THE CRITICAL CLUSTER SIZE.	34
A.	THE SILVER IODIDE SUBSTRATE	41
B.	THE SMOOTH LENNARD-JONES SUBSTRATE.	44
1.	The model	44
2.	Calculations and results.	45
a.	The critical cluster size	45
b.	The nucleation rate	50
V.	CONCLUSION	55
A.	SUMMARY OF RESULTS.	55
B.	CONCLUDING REMARKS.	58
	BIBLIOGRAPHY.	60
	VITA.	64
	APPENDICES.	65
A.	THE LENNARD-JONES PARAMETERS FOR THE K-H ₂ O INTERACTION	66
B.	THE INTERACTION POTENTIAL GRID.	68
C.	THE MONTE CARLO METHOD.	72

LIST OF ILLUSTRATIONS

Figure	Page
1 Maximal binding energies for a water molecule adsorbed on the iodine-exposed basal plane of AgI. The lines represent equipotential contours, and darker regions indicate stronger binding energies. Adjacent contours differ by 0.5 kcal/mol ¹⁴	5
2 Maximal binding energies for a water molecule adsorbed on the silver-exposed basal plane of AgI. The lines represent equipotential contours, and darker regions indicate stronger binding energies. Adjacent contours differ by 0.5 kcal/mol ¹⁴	6
3 Schematic diagram of the wurtzite structure. Large (small) circles represent iodine (silver) atoms.	11
4 The potassium impurity on the Ag-exposed basal plane of AgI. The potassium is at the center of the figure and the triangle indicates the region where the potential energy of the water monomer is minimized. The dashed circles represent the iodine atoms in the second layer.	15

Figure	Page
5 Equipotential contours for a water monomer adsorbed on the silver basal plane of AgI with a potassium impurity. Darker regions indicate stronger binding energies. Adjacent contours differ by 1.2 kcal/mol.	17
6 A three dimensional perspective of the optimal potential energy surface for a water molecule adsorbed on the silver basal plane of AgI with a potassium impurity. The K atom is located at the center of the figure.	18
7 This figure illustrates the four-layer ledge (horizontal line) on the iodine exposed basal plane of AgI and the rectangular region where the potential energy of a water molecule is minimized (cross-hatched rectangle)..	20
8 Equipotential contour plot of the optimal binding energy of a water molecule adsorbed on the iodine basal plane of AgI with a four layer ledge (dashed line). Adjacent contours differ by 2 kcal/mol.	21
9 Three dimensional perspective of the optimal potential energy of the water monomer adsorbed over the iodine basal plane of AgI with a four-layer ledge.	22

Figure	Page
10 Sites on the A) iodine exposed and B) silver exposed basal planes of AgI where the potential energy of a water molecule is minimized for several values of the effective charge assigned to the substrate atoms. Large (small) circles represent iodine (silver) atoms.	26
11 Sites on the model prism face of AgI where the potential energy of a water molecule is minimized for several values of the effective charge assigned to the substrate atoms. Values are given in Table III. Large (small) circles are I (Ag) atoms.	27
12 Comparison of average binding energies with experimental isosteric heats of adsorption q_{st} . Dashed lines represent Boltzmann weighted averages of maximal binding energies over the prism face of AgI for several values of the effective charge assigned to the substrate atoms. The average value for the optimal binding energy of the H ₂ O monomer on the model (prism) ice surface is included for reference ³⁰ . (▲)Corrin and Nelson ¹⁷ , (●)Hall and Tompkins ¹⁸ (←)Tcheurekdjian et al. ¹⁹	33
13 Plot of $-\lambda^{2/3}\langle\Delta U\rangle$ vs. $\lambda^{1/3}$ for a cluster of n = 6 water molecules at 265°K adsorbed on the basal plane of silver iodide. ²² The value of C(6) is (3/kT)(Area under the curve)..	42

Figure	Page
14 Plot of $C(n)$ vs. $n^{-1/2}$ for water adsorbed on silver iodide. The intersection of this curve with the horizontal line indicates a critical cluster size of $n^* \sim 3$ molecules for $S = 1$ at 265°K	43
15 Plot of $-\lambda^{2/3}\langle\Delta U\rangle$ vs. $\lambda^{1/3}$ for a cluster of $n = 6$ water molecules at 265°K adsorbed on the smooth Lennard-Jones substrate. The value of $C(6)$ is $(3/kT)(\text{Area under the curve})$	46
16 Plot of $C(n)$ vs. $n^{-1/2}$ for water adsorbed on the smooth Lennard-Jones substrate. The intersection of this curve with the horizontal line indicates a critical cluster size of $n^* \sim 2$ molecules for $S = 1$ at 265°K	48
17 Points on the triangle representative of the iodine-exposed basal plane of AgI where the interaction of a water molecule with the surface is calculated to create the unit cell shown in Fig. 18.	69
18 The unit rectangular cell on the iodine-exposed basal plane of AgI, obtained by reflecting the basic triangle shown at the center of the figure. The orientation of the letter "A" indicates how the reflection is performed. The bottom half of the rectangle is then reflected about the horizontal (dashed) line to obtain the full unit cell.	70

Figure	Page
19 Flow chart of the Metropolis Monte Carlo method.	73
20 Average binding energy as a function of the number of Monte Carlo steps for $n = 6$ molecules adsorbed on the smooth Lennard-Jones substrate.. . . .	74
21 Average value of ΔU as a function of the number of Monte Carlo steps for $n = 6$ water molecules adsorbed on the smooth Lennard-Jones substrate.. . . .	76

LIST OF TABLES

Table	Page
I Comparison of the minimized values of the potential energy $V(q')$ (column 3), with the approximate values obtained from $\langle X \rangle \cdot V(.6)$ (column 5), for the sites shown in Fig. 10 A), on the iodine exposed basal plane of AgI. Units are kcal/mol and ΔV is $\langle X \rangle V(.6) - v(q')$	28
II Comparison of the minimized values of the potential energy $V(q')$ (column 3) with the approximate values obtained from $\langle X \rangle \cdot V(.6)$ (column 5) for the sites shown in Fig. 10 B) on the silver exposed basal plane of AgI. Units are kcal/mol and ΔV is $\langle X \rangle V(.6) - V(q')$	29
III Comparison of the minimized values of the potential energy $V(q')$ (column 3) with the approximate values obtained from $\langle X \rangle \cdot V(.6)$ (column 5) for the sites indicated in Fig. 11, for the AgI prism face. Units are kcal/mol and ΔV is $\langle X \rangle V(.6) - V(q')$	30

Table

Page

- IV Calculated values of $C(n)$ for water molecules adsorbed on the smooth Lennard-Jones substrate. The uncertainties reflect the maximum and minimum areas under the curves of $-\lambda^{2/3} \langle \Delta U \rangle$ vs $\lambda^{1/3}$ (see Fig. 15 for $n=6$). The value of $C(5)$ was estimated from a curve fit and thus no error bars are available. The results for $n = 44$ were not run long enough to specify error bars. 47
- V This table shows the free energy of formation (column 6) for a cluster of size n (column 1), calculated from Eq.(20). Columns 2-5 give the quantities that enter into this equation. (Note that the free energy of formation for $n = 24$ and 44 are not given in this table. In order to calculate $\Delta F(n)/kT$ from Eq. (20) all $C(i)$ from $i = 2$ to n must be determined.) 52

I. INTRODUCTION

A. MOTIVATION FOR THIS WORK

It is well known that ice plays a dominant role in precipitation processes of midlatitude continental clouds.¹⁻⁴ The upper regions of such clouds are generally composed of a relatively stable supercooled (0 to -30 °C) water droplet size distribution. The stability of the system reduces the probability of droplet growth and in most cases prohibits the onset of precipitation. However, small ice crystals in the same environment are unstable (because of the lower vapor pressure for ice below 0 °C) and grow at the expense of the water molecules given off by the supercooled water droplets. Thus whereas the supercooled water droplets are restricted in size, the ice aggregates can become massive enough to fall through the cloud and grow via collisions with supercooled water droplets and other ice crystals in the cloud. Depending on the cloud dynamics and the temperature profile of the cloud, the falling ice particles can fall from the cloud base as snow, hail, sleet or rain. This role of ice in initiating the precipitation process (called the Bergeron process³) is believed to be responsible for most precipitation in midlatitude continental clouds where the cloud condensation nuclei (hygroscopic foreign particulates) are numerous and small. The latter leads to a high

concentration of small cloud water droplets. In other clouds (for example marine clouds) the cloud condensation nuclei can be large (greater than 1 micron) and produce a smaller concentration of large, unstable cloud water droplets. The latter provides conditions favorable for precipitation via coalescence of the water droplets. Thus the nucleation of ice is a process central to the understanding of cloud microphysics in midlatitude continental clouds.

The nucleation rate, J , and the threshold temperature for ice nucleation under cloud conditions are the quantities most readily applied to cloud modelling and "cloud seeding" experiments. The nucleation rate is the number of embryos of the new phase (ice) formed from the parent phase (liquid or vapor) per unit volume per unit time. The threshold temperature is generally interpreted to be that temperature (under the specified water vapor pressure) which produces a nucleation rate of one embryo per cm^3 per second. The most widely used theories of homogeneous and heterogeneous nucleation⁴⁻⁶ of water and ice were developed about forty years ago and suffer from conceptual difficulties. A basic assumption of both theories is that macroscopic densities and bulk interface free energies are valid for water embryos that contain on the order of 100 molecules or less. For the case of heterogeneous nucleation^{7,8}, the substrate is considered to be completely homogeneous, i.e., the substrate has no localized surface features such as structure, defects, or

preferred adsorption sites. It has been found experimentally^{4,8}, however, that substances known to be hydrophobic are excellent ice nucleating agents. This is thought to be a consequence of the existence of localized hydrophilic sites on the surface, where water molecules tend to be adsorbed and facilitate the nucleation of a water droplet.

Silver iodide (AgI) has been extensively used in cloud seeding since it was proposed and identified as an effective ice nucleating agent by the experiments of Vonnegut⁹ in 1947. The β -form of AgI has a wurtzite structure similar to that of ice I_h with a small lattice mismatch on both the basal and prism faces ($\sim 2\%$)¹⁰. It is believed that these similarities with ice I_h are in part responsible for the ice nucleating properties of silver iodide. On the other hand, it has been determined that contaminated silver iodide is a more efficient ice nucleant than the pure form¹¹. This may be due to an increase of preferred adsorption sites such as chemical impurities or the presence of faults (dislocations, ledges).

In this study we propose to investigate what effect the substrate features (impurities, defects, and surface structures) mentioned above have on the maximal binding energy surfaces of a water monomer on a model basal plane of AgI, and to extend these studies to adsorbed water clusters on model substrates with and without defects.

B. SUMMARY OF PREVIOUS STUDIES OF H₂O ON AgI

In an effort to understand the role of nucleating agents on the formation of ice, theoretical studies began with the modelling of a single water molecule interacting with model silver iodide surfaces.^{12,13} (See also the Ph.D. thesis of J.Kiefer¹⁴). First, the interaction potential of a water molecule with the iodine and silver atoms in the substrate was modelled by a pair-interaction potential containing electrostatic, Lennard-Jones, and induction terms. A computer program was designed to generate the maximal binding energy surfaces for the water monomer on the model (rigid) AgI substrate. This was done for representative regions of the prism and hexagonal basal faces of the model substrate.¹²⁻¹⁴

Sample results of these previous studies are shown in Figs. 1 and 2, as equipotential contours; the darker regions indicate stronger binding energies. On the basal planes the preferred bonding sites form a pattern with approximate six-fold symmetry around the exposed substrate atom. This suggests that water molecules tend to be adsorbed around an exposed substrate atom with hexagonal symmetry¹². Although the water-water interaction has not been taken into account, the six-fold sites are approximately the same distance apart as in hexagonal ice ($\approx 2.8 \text{ \AA}$).

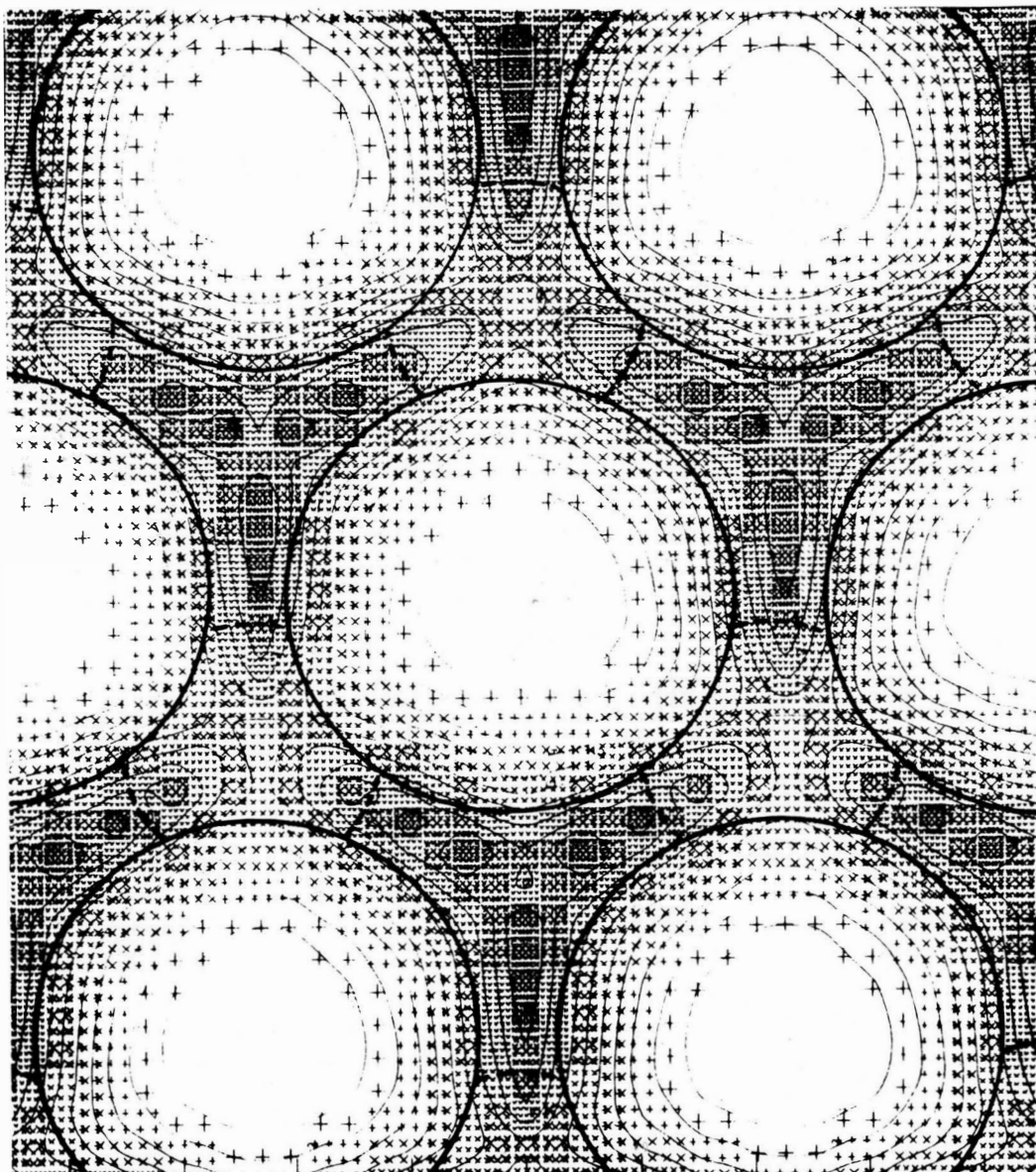


Fig. 1. Maximal binding energies for a water molecule adsorbed over the iodine-exposed basal plane of AgI. The lines represent equipotential contours, and darker regions indicate stronger binding energies. Adjacent contours differ by 0.5 kcal/mol.¹⁴

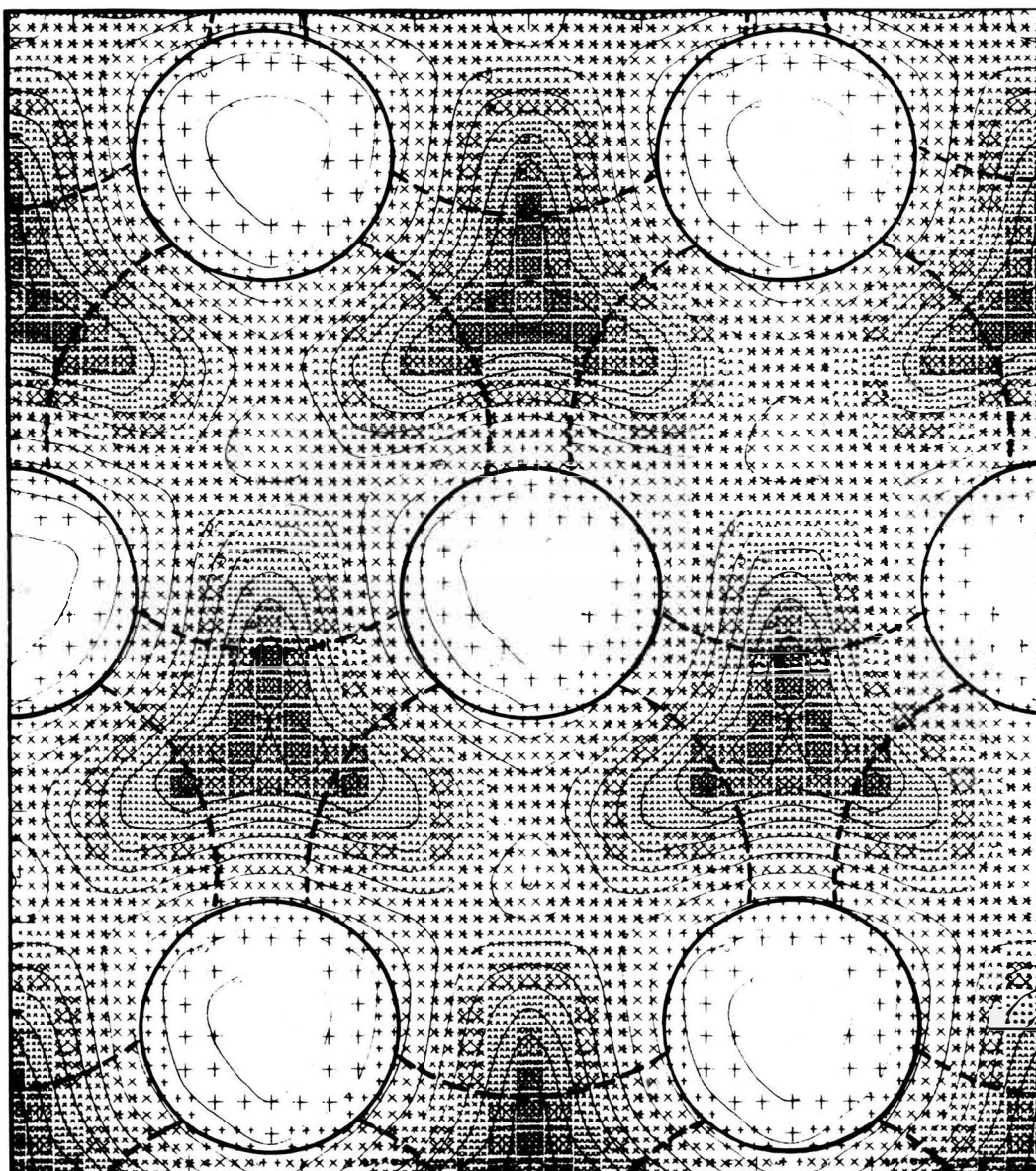


Fig. 2. Maximal binding energies for a water molecule adsorbed on the silver-exposed basal plane of AgI. The lines represent equipotential contours, and darker regions indicate stronger binding energies. Adjacent contours differ by $0.5 \text{ kcal/mol}^{14}$.

C. DISCUSSION OF THE PRESENT WORK

Defects are thought to play a role in the ice-nucleating process on surfaces. Hence, as a continuation of these studies, we investigate the interaction of a single water molecule with a potassium impurity on the Ag-exposed basal plane, and above a four-layer ledge¹⁵ on the I-exposed basal plane. This study is discussed in section II.

The previous studies¹²⁻¹⁴ use an effective charge for the Ag and I substrate ions of 0.6 e. This value was taken from the work of Buhrer et al.¹⁶. No attempt was made to alter this effective charge. However, the average binding energy to the model prism AgI substrate for the water monomer found in the studies mentioned above, is 20 kcal/mole¹². This is high when compared to experimental results for physical adsorption^{17,18,19} of water on silver iodide. The value of the binding energy depends strongly on the effective charge assigned to the substrate atoms. A study is made of the average value of the binding energy as a function of the effective charge Q . Comparison with the results of Refs. 17-19 indicates that $Q = 0.4 e$ gives a reasonable value (~10 kcal/mol) for the average H₂O-substrate binding energy. This study is discussed in section III.

The next step in this investigation is to include the water-water interaction and to study the effect of the substrate on the structure and stability of water clusters¹⁵.

For this purpose a Metropolis²⁰ Monte Carlo method is used. The Monte Carlo (MC) method requires the evaluation of the interaction potential between a water molecule and the AgI substrate on the order of 10^6 times. A judicious use of available computer time rules out the direct calculation of the total interaction potential at every MC step. To circumvent this problem, a grid of H_2O -AgI potential values is created over a unit rectangle representative of the surface from a height of 0.1 Å to 5 Å above the substrate in steps of 0.1 Å (see Appendix B). If a molecule is within this range, a linear interpolation is made for the interaction potential. For H_2O -substrate separations between 5 and 10 Å a six-point Lagrange interpolation is made using average values of the potential over the unit rectangle, calculated in steps of 1 Å. Above 10 Å the interaction of the water molecule with the substrate is assumed to be negligible. A grid is also used for the H_2O - H_2O interactions. For these studies we use the revised central force potentials of Stillinger and Rahman²¹.

The Monte Carlo method is also used to study the critical cluster size²² for water clusters on substrates such as the basal plane of AgI and a smooth plane with a Lennard-Jones potential. The critical cluster size is the number of molecules in a cluster that has equal probability of gaining or losing a molecule. Clusters containing more molecules than the critical size will grow at the expense of the surrounding water monomers and become macroscopic water droplets. The

critical cluster size (n^*) can be related to the nucleation rate J , the number of water droplets nucleated per cm^2 per second. The quantity J can be used to predict threshold temperatures for nucleation. The latter can be measured experimentally and provides a test of the model. These studies are discussed in section IV.

II. THE BASAL PLANES OF AgI WITH DEFECTS

In this section we discuss the calculation of the maximal binding energy surfaces of a water monomer over the Ag-basal plane with a potassium impurity and over the I-basal plane with a four-layer ledge.

A. THE POTASSIUM IMPURITY

1. The model substrate and the interaction potentials.

The AgI substrate is modelled as an infinite array of point charge atoms in the wurtzite structure (Fig. 3). The lattice parameters are $a = 4.58 \text{ \AA}$ and $c = 7.49 \text{ \AA}$ and an effective charge of $0.6 e$ is used.¹⁴ The water molecule is represented by the four point charge ST-2 model of Stillinger²³ and remains rigid in the calculations. The AgI substrate is also assumed to be rigid. The H_2O -AgI effective interaction potential is described by Hale and Kiefer¹², and is given by:

$$V = V_{lj} + V_{el} + V_{ind} \quad (1)$$

where

$$V_{lj} = \sum_m 4\epsilon_{mW} (x^{12} - x^6) \quad (\text{with } x \equiv \sigma_{mW} / |\underline{r}_0 - \underline{r}_m|), \quad (2)$$

$$V_{el} = 1/2 \sum_i \sum_m Q_i Q_m / |\underline{r}_i - \underline{r}_m|, \quad (3)$$

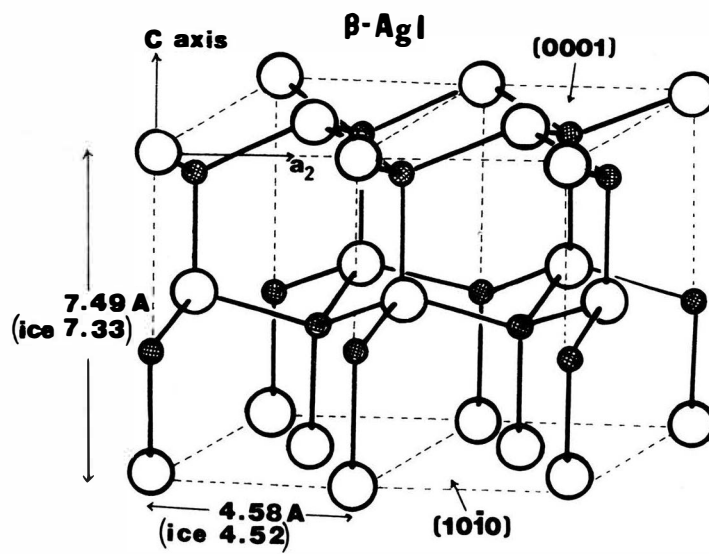


Fig. 3. Schematic diagram of the wurtzite structure.
Large (small) circles represent iodine (silver) atoms.

and

$$V_{\text{ind}} = -1/2 \sum_n \sum_m \alpha_w Q_n Q_m \frac{(\underline{r}_0 - \underline{r}_n) \cdot (\underline{r}_0 - \underline{r}_m)}{|\underline{r}_0 - \underline{r}_n|^3 |\underline{r}_0 - \underline{r}_m|^3}$$

$$-1/2 \sum_n \sum_i \sum_j \alpha_n Q_i Q_j \frac{(\underline{r}_i - \underline{r}_n) \cdot (\underline{r}_j - \underline{r}_n)}{|\underline{r}_i - \underline{r}_n|^3 |\underline{r}_j - \underline{r}_n|^3} \quad (4)$$

Here the n and m sums are over the surface Ag and I atoms; i and j sums run over the four charges of the water molecule. Q_n , α_n , \underline{r}_i , and \underline{r}_n are the effective charge, polarizability, and position vector of the i^{th} charge in the H_2O model and the n^{th} atom in the AgI substrate; Q_i , α_w , and \underline{r}_0 are the i^{th} ST-2 charge, polarizability, and center of mass position vector of the water molecule, respectively.

The following values were used for the parameters in the potential function (see Appendix A):^{12,14}

$$\begin{aligned} \sigma_{\text{AgW}} &= 3.171 \text{ A}, & \epsilon_{\text{AgW}} &= 0.5467 \text{ kcal/mol}, \\ \sigma_{\text{IW}} &= 3.342 \text{ A}, & \epsilon_{\text{IW}} &= 0.686 \text{ kcal/mol}, \\ \alpha_{\text{Ag}} &= 2.40 \text{ A}^3, & \alpha_{\text{I}} &= 6.43 \text{ A}^3, \\ \alpha_{\text{W}} &= 1.44 \text{ A}^3, & Q_{\text{Ag}} &= 0.6 e, Q_{\text{I}} = -0.6 e. \end{aligned}$$

In the model for the water molecule, there are four point charges (two negative and two positive of magnitude $Q = 0.24 e$) arranged along tetrahedral directions from the center of mass. The positive charges are 1.0 A and the negative charges are 0.80 A from the center of mass.

The summation in Eq. 2 is taken over atoms lying within a radius of 16 Å; the same cutoff is used for the summations in Eq. 4. In the latter equation the double summation over m and n is reduced to the $m = n$ terms. Contribution from $m \neq n$ was found to be less than 10 % of the total contribution from V_{ind} .¹⁴ The summation in Eq. 3 is done partially in direct lattice space and partially in reciprocal lattice space. These procedures are described in detail in reference 14.

The modification for the basal plane with a potassium impurity is made by replacing one of the surface silver atoms with a point charge of 0.95 e and by adding one third of the unbalanced charge ($-0.35 e$) to each of the three neighboring iodine atoms. The latter procedure ensures that the surface has no net charge. A value of 0.95 e for the effective charge of the potassium is suggested by the larger ionicity of KI (0.95 compared to 0.77 for AgI).²⁴ This choice of effective charge for K is viewed as part of the model, and is intended to represent a site on the AgI surface with altered charge distribution. For the short-range potential V_{lj} , $\epsilon_{KW} = 0.45$ kcal/mol and $\sigma_{KW} = 3.04$ Å are used; all the other parameters are as given above except for the effective charge of the three neighboring iodine atoms. The values of ϵ and σ for the potassium-water interaction potential are obtained from those of argon and water^{25,26} using the standard formulas prescribed by Hirschfelder²⁷. This calculation is described in Appendix A. The ionic polarizability of potassium ($\alpha_K^+ = 1.33 \text{ Å}^3$)²⁸ is used in the potentials in Eq. 4.

2. Calculations and results. In order to generate an optimal binding energy surface of the water molecule adsorbed over the K impurity, a grid of points about 0.25 Å apart was marked off in the triangular region indicated in Fig. 4. This equilateral triangle with one vertex on the potassium impurity is 5.82 Å on a side and is enlarged from that used in generating the optimal binding energy surfaces on the smooth AgI substrate. The procedure is to fix the center of mass projection of the adsorbed molecule above the grid point (x, y) and minimize the potential function V , by varying the surface- H_2O distance, z , and the Euler angles of the water molecule relative to the surface plane. The energy surface is thus a four dimensional surface at each (x, y) point and has a complicated dependence on the variables. The minimization routine used is VAO4A of the Harwell subroutine library²⁹. The results of the triangle are used to generate an optimal potential energy contour for the hexagonal region shown in Fig. 4. Beyond the edges of the hexagon, the optimal potential energy for the adsorbed water molecule is approximated by the values for the smooth silver basal plane obtained in previous calculations¹⁴. At the edges of the hexagon, the optimal potential energies obtained from the potassium impurity calculations and the smooth surface results differ by less than 10 %. The resulting two dimensional contour density plot of the optimal binding energy of the adsorbed water molecule above the site is shown

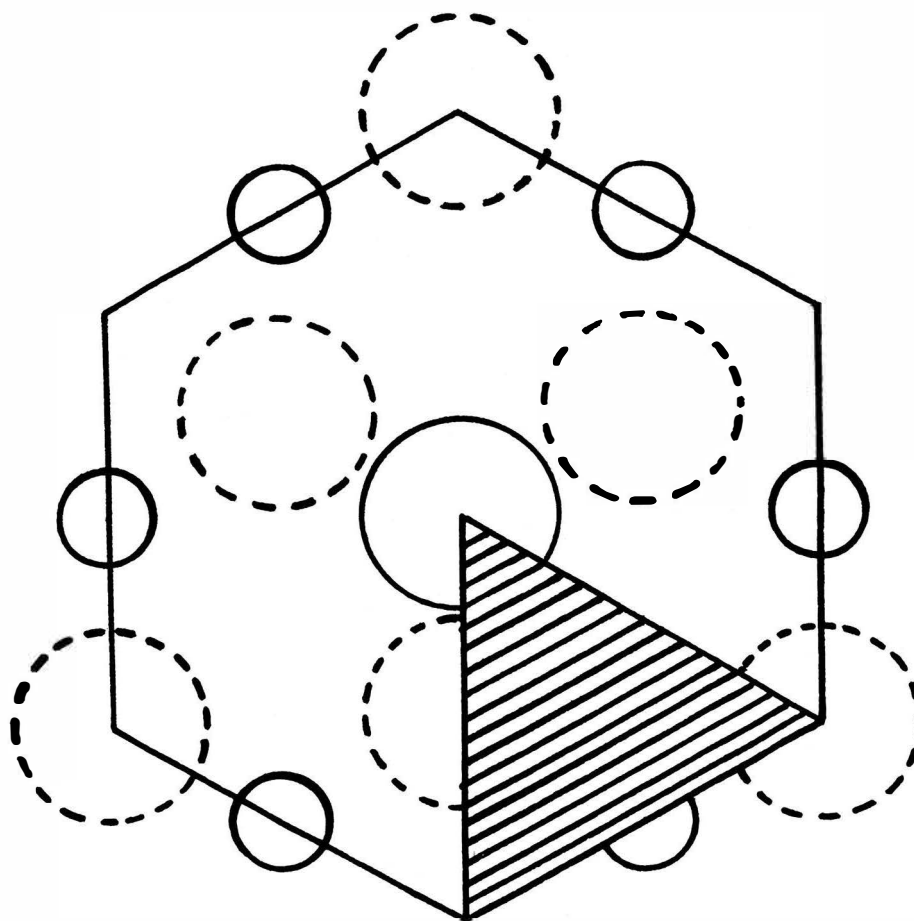
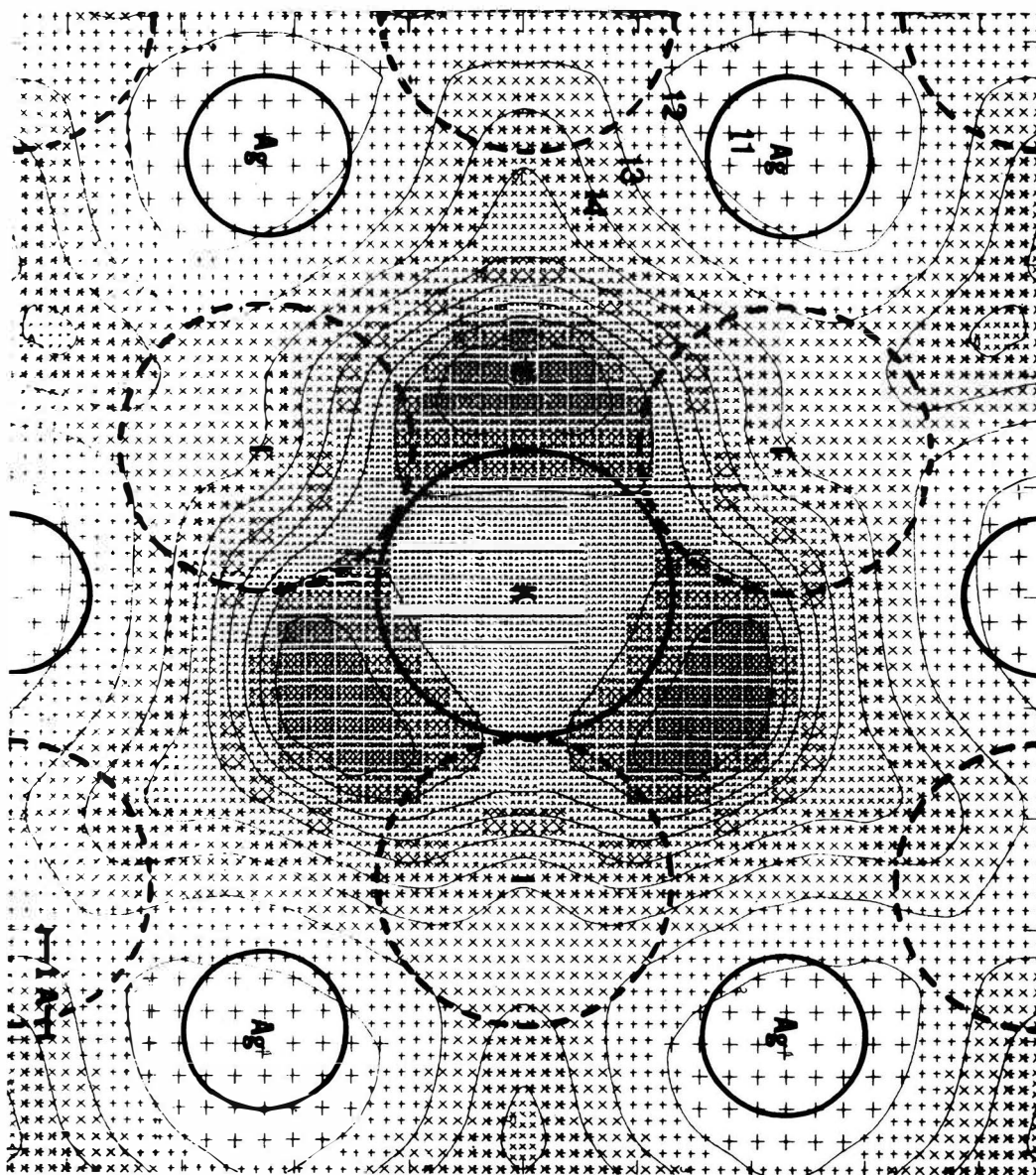


Fig. 4. The potassium impurity on the Ag-exposed basal plane of AgI. The potassium is at the center of the figure and the triangle indicates the region where the potential energy of the water monomer is minimized. The dashed circles represent the iodine atoms in the second layer.

in Fig. 5. The contours represent lines of equal maximal binding energy and larger binding energies are indicated by the more heavily shaded regions. A three dimensional perspective view of the optimal potential energy (the negative of the optimal binding energy) is shown in Fig. 6. The energy surface near the edges of the contour (beyond the edges of the hexagon indicated in Fig. 4) is that obtained for the smooth basal surface of AgI; the figure shows no appreciable discontinuity at the edges of the hexagon, and the impurity at the center shows a pronounced effect.

Directly over the K impurity, the optimal binding energy of the adsorbed water molecule is 18 kcal/mol compared to 11 kcal/mol over the silver atom on the smooth substrate. At the favored adsorption sites indicated by the darkest regions in Fig. 5, the optimal binding energy is between 22 and 23 kcal/mol. This is about 40 % larger than the optimal binding energy at the preferred (interstitial) adsorption sites on the smooth substrate. As is evident in Fig. 5, the interstitial binding sites near the central atom have been drawn toward the K impurity and the symmetrical pattern of the smooth surface energy contour is distorted.

Fig. 5. Equipotential contours for a water monomer adsorbed on the silver basal plane of AgI with a potassium impurity. Adjacent darker regions indicate stronger binding energies. Equipotential contours differ by 1.2 kcal/mol.



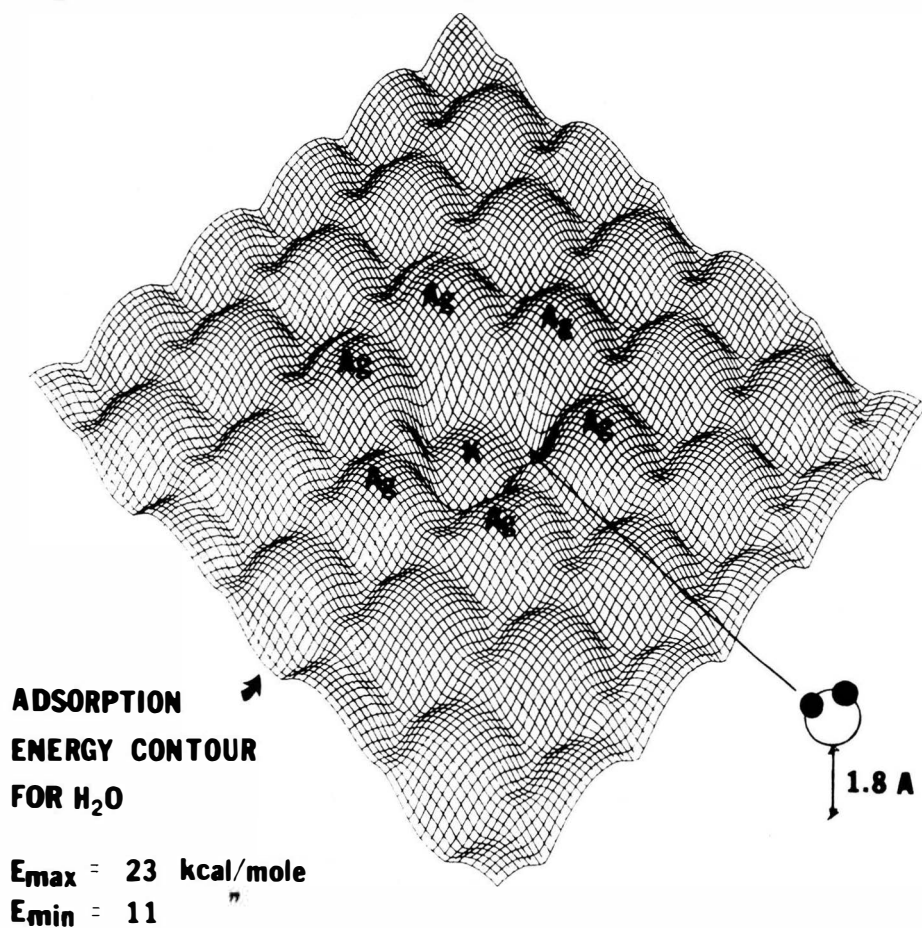
H₂O ADSORPTION SITES - AgI BASAL FACE WITH K IMPURITY

Fig. 6. A three dimensional perspective of the optimal potential energy surface for a water molecule adsorbed on the silver basal plane of AgI with a potassium impurity. The K atom is located at the center of the figure.

B. THE FOUR-LAYER LEDGE

The substrate for this study is obtained from the smooth AgI basal plane with the iodines exposed by removing four atomic layers from half of the semi-infinite array. The ledge is parallel to the horizontal line in Fig. 7, and the height of the ledge is 7.49 Å. This corresponds to the height of a unit cell in AgI. The center of mass projection of the adsorbed water molecule is fixed over a grid of points about 0.25 Å apart on a rectangle of dimensions 2.29 Å x 16 Å (Fig. 7). The center of mass-surface separation distance and the Euler angles of the water molecule are varied at each grid point to obtain the maximal binding energy at each grid point. Values for a larger region of the surface can be obtained by reflecting and translating the values from the "unit rectangle". At the edges of the rectangle parallel to the ledge, the values from the rectangle are matched to those of the undisturbed substrate; differences are less than 10 %. A two dimensional contour density plot similar to Fig. 5 is shown in Fig. 8 for the optimal binding energy of the adsorbed water molecule above the four-layer ledge. Fig. 9 is a three dimensional perspective view of the optimal potential energy surface corresponding to Fig. 6. The structure of the ledge is indicated, together with values of the optimal binding energy at specific sites¹⁵.

Along a region parallel to the edge of the step, the optimal binding energy is increased to 23 kcal/mol from

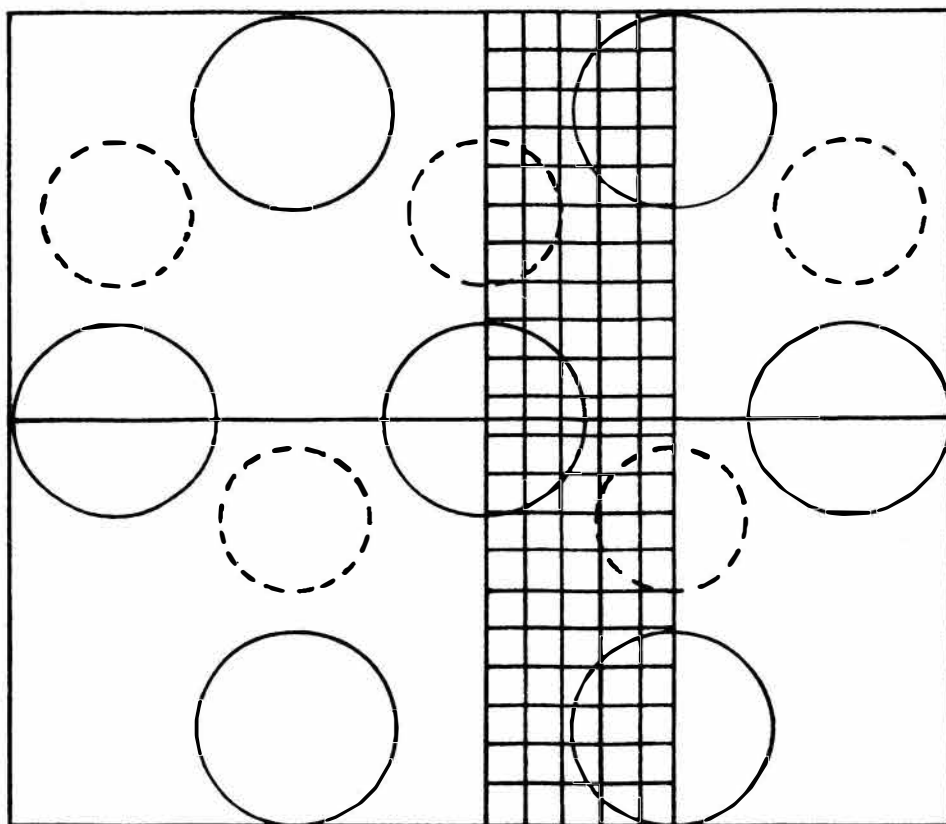


Fig. 7. This figure illustrates the four-layer ledge (horizontal line) on the iodine exposed basal plane of AgI and the rectangular region where the potential energy of a water molecule is minimized (cross-hatched rectangle).

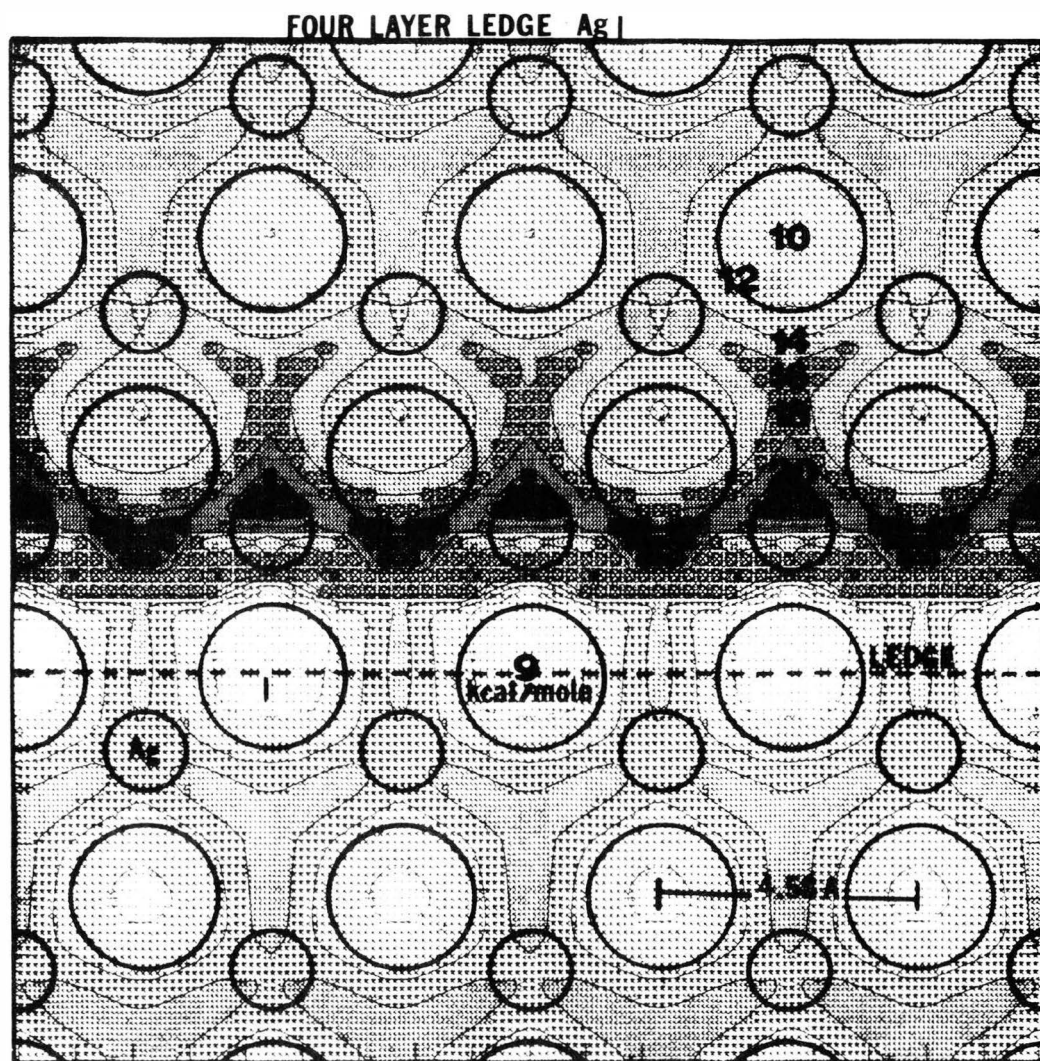


Fig. 8. Equipotential contour plot of the optimal binding energy of a water molecule adsorbed on the iodine basal plane of AgI with a four-layer ledge (dashed line). Adjacent contours differ by 2 kcal/mol.

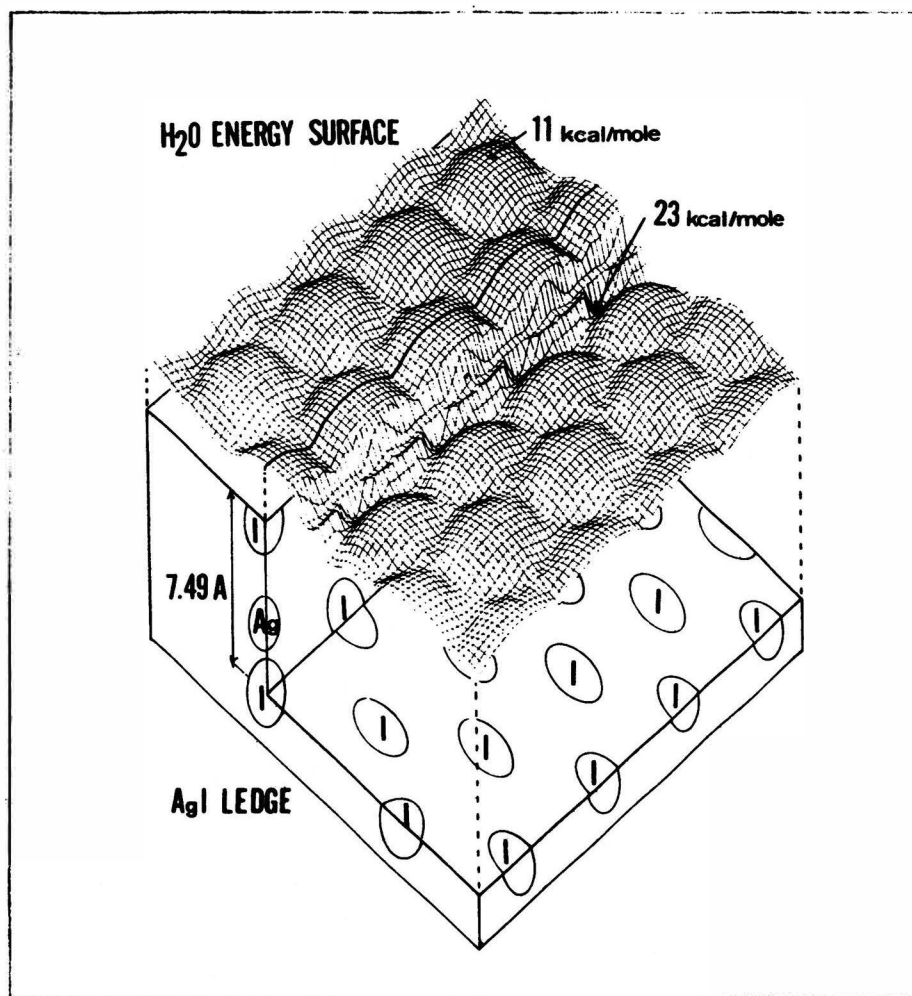


Fig. 9. Three dimensional perspective of the optimal binding energy of the water monomer adsorbed over the iodine basal plane of AgI with a four-layer ledge.

typical values of 16 kcal/mol at interstitial sites on the smooth basal surface. Favored sites on the smooth prism face of AgI found in a previous study^{12,14} are about 20 kcal/mol. Thus the increased binding energy near the four-layer ledge is not due exclusively to the exposed prism face of the ledge, but arises in part from multiple bonding of the water with atoms in the basal and prism faces at the bottom of the step. The maximal binding energy sites for the water molecule near the step are displaced about 2.5 Å from the physical edge of the ledge. Because of the multiple bonding sites parallel to the prism face of the ledge the energy surface displays some discontinuity as the water molecule makes the transition from the upper terrace to the lower terrace. In Fig. 8 the upper part of the figure corresponds to the lower terrace and the physical edge of the step is along the dashed line. On the lower terrace the water molecule feels the effect of the ledge over larger horizontal distances. On the upper terrace, the ledge distorts the binding energy surface of the adsorbed water molecule only slightly. The primary distortion on the upper terrace is at the physical line of the step where the maximal binding energies are decreased by about 20 % from those found at corresponding sites on the smooth iodine basal plane. The effect appears to be due to a reduced number of nearest neighbors for the adsorbed H₂O as it nears the edge of the step on the upper terrace. Kiefer^{12,14} has calculated the energy surface for a two-layer ledge. A comparison of his

results with the four-layer ledge results indicates that a four-layer step is just high enough to detect effects of multiple bonding at the base of the ledge . The two-layer ledge¹⁴ produced maximal binding energies at the step of about 21 kcal/mol, barely larger than the prism face itself (20 kcal/mol). Kiefer's and this study also suggest that two- and four-layer ledges (which must be prominent features of a macroscopically smooth basal face) introduce adsorption sites on the basal face which are about as active as those on the prism face. The present calculation also suggests that larger steps, say six or more atomic layers, might not produce adsorption sites significantly more active than the four-layer ledge. This is indicated by the location of the maximal binding sites at the bottom of the ledge. Increasing the height of the step should not alter the number of nearest neighbor bonds available at the bottom of the ledge, and as the step height increases the central region should take on features of the prism face.

III. THE BINDING ENERGY AS A FUNCTION OF EFFECTIVE CHARGE

In this section we discuss the optimal binding energy of a water molecule adsorbed on the basal and prism faces of AgI for several values of the effective charge assumed for the ions in the substrate, and a comparison is made with experimental results. This indicates that a judicious choice for the effective charge of the substrate is $Q = 0.4 e$.

A. MAXIMAL BINDING ENERGY AS A FUNCTION OF CHARGE

The potential energy is minimized with the VAO4A²⁹ routine for values of the effective charge of 0.3, 0.4, and 0.5 e assigned to the substrate atoms over both basal planes and the prism face of AgI. To avoid the expense involved in minimizing the potential energy over the whole triangle representative of the of the basal planes (Fig. 10), and the rectangle representative of the prism face (Fig. 11), a study is made of the potential energy minima at some arbitrarily selected sites indicated in Figs. 10 and 11, and the results are given in Tables I, II, and III. Column 4 of these tables shows that the ratio X of the computed value of the optimal binding energy for a charge q' to the corresponding value at $q = 0.6 e$, is nearly constant for all sites, being a function of q' only. The average value of this ratio over the sites mentioned, $\langle X(q') \rangle \equiv \langle V(q')/V(q) \rangle$, is calculated for each charge q' and a value of $V(q')$ is then approximated by $V(q') \sim$

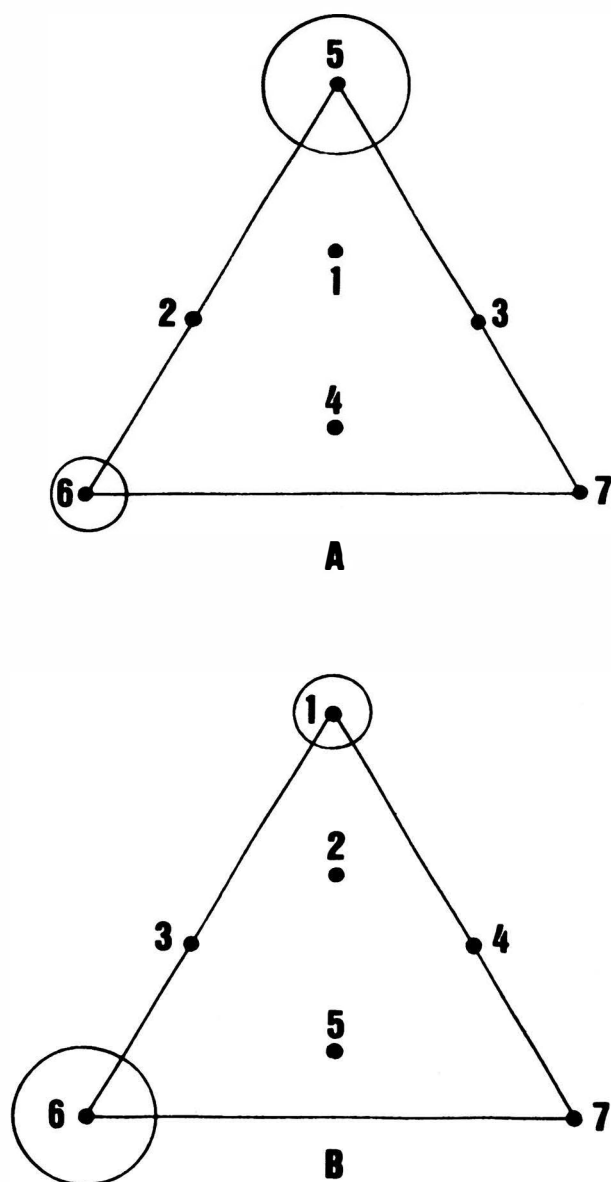


Fig. 10. Sites on the A) iodine exposed and B) silver exposed basal planes of AgI where the potential energy of a water molecule is minimized for several values of the effective charge assigned to the substrate atoms. Large (small) circles represent iodine (silver) atoms.

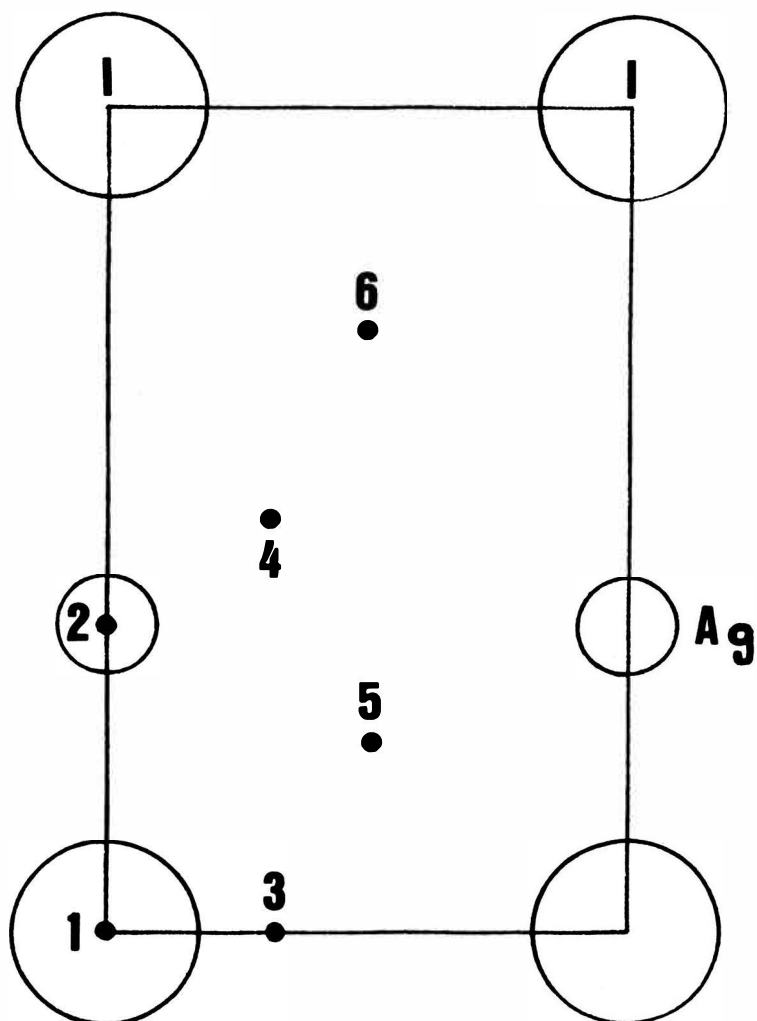


Fig. 11. Sites on the model prism face of AgI where the potential energy of a water molecule is minimized for several values of the effective charge assigned to the substrate atoms. Values are given in Table III. Large (small) circles are I (Ag) atoms.

TABLE I

Comparison of the minimized values of the potential energy $V(q')$ (column 3) with the approximate values obtained from $\langle X \rangle \cdot V(.6)$ (column 5), for the sites shown in Fig. 10 A), on the iodine exposed basal plane of AgI. Units are kcal/mol and ΔV is $\langle X \rangle V(.6) - V(q')$.

SITE #	V(.6)	V(.5)	X	$\langle X \rangle V(.6)$	ΔV
1	11.214	9.286	0.828	9.364	0.078
2	11.987	9.981	0.833	10.009	0.028
3	12.314	10.223	0.830	10.282	0.059
4	14.833	12.385	0.835	12.385	0.000
5	9.734	8.052	0.827	8.128	0.076
6	13.280	11.280	0.849	11.089	-0.191
7	15.038	12.683	0.843	12.557	-0.126

SITE #	V(.6)	V(.4)	X	$\langle X \rangle V(.6)$	ΔV
1	11.214	7.584	0.676	7.738	0.154
2	11.987	8.211	0.685	8.271	0.060
3	12.314	8.381	0.681	8.497	0.116
4	14.833	10.231	0.690	10.235	0.004
5	9.734	6.568	0.675	6.716	0.148
6	13.280	9.536	0.718	9.163	-0.373
7	15.038	10.621	0.706	10.376	-0.245

SITE #	V(.6)	V(.3)	X	$\langle X \rangle V(.6)$	ΔV
1	11.214	6.099	0.544	6.325	0.226
2	11.987	6.665	0.556	6.761	0.097
3	12.314	6.773	0.550	6.945	0.172
4	14.833	8.354	0.563	8.366	0.012
5	9.734	5.275	0.542	5.490	0.215
6	13.280	8.034	0.605	7.490	-0.544
7	15.038	8.849	0.588	8.481	-0.368

TABLE II

Comparison of the minimized values of the potential energy $V(q')$ (column 3) with the approximate values obtained from $\langle X \rangle \cdot V(.6)$ (column 5) for the sites shown in Fig. 10 B) on the silver-exposed basal plane of AgI. Units are kcal/mol and ΔV is $\langle X \rangle V(.6) - V(q')$.

SITE #	V(.6)	V(.5)	X	$\langle X \rangle V(.6)$	ΔV
1	10.797	8.836	0.818	8.951	0.115
2	11.754	9.644	0.820	9.744	0.100
3	12.339	10.198	0.826	10.229	0.031
4	12.838	10.572	0.823	10.643	0.071
5	14.657	12.176	0.831	12.151	-0.025
6	12.028	10.147	0.844	9.971	-0.176
7	15.499	13.041	0.841	12.849	-0.192

SITE #	V(.6)	V(.4)	X	$\langle X \rangle V(.6)$	ΔV
1	10.797	7.111	0.659	7.342	0.231
2	11.754	7.791	0.663	7.993	0.202
3	12.339	8.321	0.674	8.390	0.069
4	12.838	8.582	0.668	8.730	0.148
5	14.657	10.005	0.683	9.967	-0.038
6	12.028	8.510	0.708	8.179	-0.331
7	15.499	10.910	0.704	10.539	-0.371

SITE #	V(.6)	V(.3)	X	$\langle X \rangle V(.6)$	ΔV
1	10.797	5.614	0.520	5.949	0.335
2	11.754	6.185	0.526	6.476	0.291
3	12.339	6.698	0.543	6.799	0.101
4	12.838	6.856	0.534	7.074	0.218
5	14.657	8.128	0.554	8.076	-0.052
6	12.028	7.109	0.591	6.627	-0.482
7	15.499	9.084	0.586	8.540	-0.544

TABLE III

Comparison of the minimized values of the potential energy $V(q')$ (column 3) with the approximate values obtained from $\langle X \rangle \cdot V(.6)$ (column 5) for the sites indicated in Fig. 11, for the AgI prism face. Units are kcal/mol and ΔV is $\langle X \rangle V(.6) - V(q')$.

SITE #	V(.6)	V(.5)	X	$\langle X \rangle V(.6)$	ΔV
1	5.976	4.976	0.833	4.888	-0.088
2	6.683	5.517	0.826	5.467	-0.050
3	7.080	5.865	0.828	5.791	-0.074
4	9.614	7.838	0.815	7.864	0.026
5	19.755	15.282	0.774	16.160	0.878
6	14.873	12.403	0.834	12.166	-0.237

SITE #	V(.6)	V(.4)	X	$\langle X \rangle V(.6)$	ΔV
1	5.976	4.151	0.695	4.004	-0.147
2	6.683	4.567	0.683	4.478	-0.089
3	7.080	4.870	0.688	4.744	-0.126
4	9.614	6.366	0.662	6.441	0.075
5	19.755	11.831	0.599	13.236	1.405
6	14.873	10.321	0.694	9.965	-0.356

SITE #	V(.6)	V(.3)	X	$\langle X \rangle V(.6)$	ΔV
1	5.976	3.491	0.584	3.305	-0.186
2	6.683	3.821	0.572	3.696	-0.125
3	7.080	4.087	0.577	3.915	-0.172
4	9.614	5.179	0.539	5.316	0.137
5	19.755	9.205	0.466	10.924	1.719
6	14.873	8.612	0.579	8.225	-0.387

$\langle X \rangle \cdot V(0.6)$ for each site studied. These values are given in column 5 of the above tables, and column 6 shows ΔV , the difference between the actual maximal binding energy at the site and the value generated by using $\langle X \rangle V(.6)$.

Examination of ΔV suggests that for the purposes at hand one can avoid the considerable computer expense and time required to minimize the potential energy at every point of the grid for each of the faces and different charges. For a given point P in the triangle (rectangle) for the basal (prism) face, the value of the potential energy at that point $V(P, q')$ is approximated by $\langle X(q') \rangle \cdot V(P, 0.6)$. Maximal binding energy surfaces for the water molecule are obtained in this manner (from the energy surfaces for $q = 0.6$) for $q' = 0.3 e$, $0.4 e$, and $0.5 e$ and Boltzmann weighted averages over these surfaces are calculated for comparison with experiment. This comparison is presented in section B.

B. COMPARISON OF AVERAGE BINDING ENERGIES WITH EXPERIMENT

A comparison of our calculations with experimental results is possible if one considers isosteric (constant specific surface area) heats of adsorption in the limit of low coverage. In this limit the isosteric heat of adsorption corresponds to the binding energy of a molecule adsorbed on the substrate. The measurements of Corrin and Nelson¹⁷, Hall and Tompkins¹⁸, and Tcheurekdjian et al.¹⁹ of the isosteric heats of adsorption for water adsorbed on AgI are shown in Fig. 12. The dashed lines indicating the average value of the maximal binding energy over the rectangle representative of the prism face for 0.3, 0.4, 0.5, and 0.6 e. The dashed line labeled "ice" is the average maximal binding energy of the water molecule on the model prism face of ice³⁰. These averages are calculated as Boltzmann weighted sums of the maximal binding energy over the surface. Fig. 12 shows a broad spectrum of experimental results for low coverages, with heats of adsorption differing by about 10 kcal/mol. Since we only want the model to give reasonable values for the H₂O-AgI binding energy which are comparable to those of H₂O on ice, it is considered that a judicious choice for the effective charge of the substrate atoms is $Q = 0.4$ e. Fig. 12 shows that for this value of Q the average maximal binding energy is bracketed by the experimental results and lies close to the average value of H₂O on the prism face of ice. This value of Q will be used in all subsequent calculations.

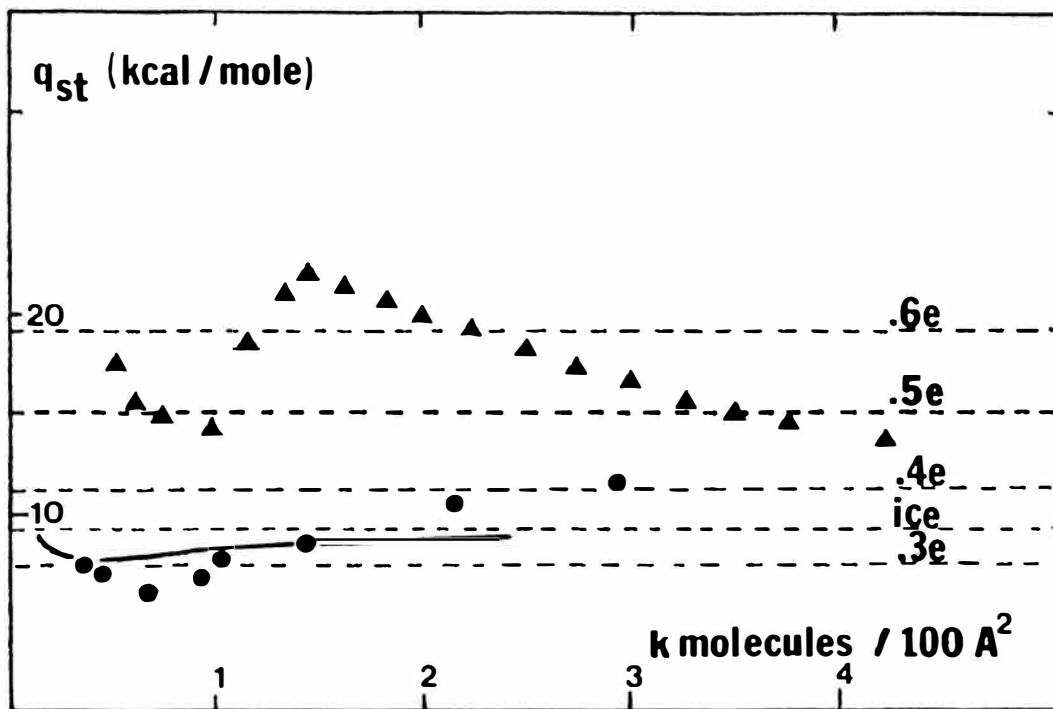


Fig. 12. Comparison of average binding energies with experimental isosteric heats of adsorption q_{st} . Dashed lines represent Boltzmann weighted averages of maximal binding energies over the prism face of AgI for several values of the effective charge assigned to the substrate atoms. The average value for the optimal binding energy of the H_2O monomer on the model (prism) ice surface is included for reference.³⁰
 (▲)Corrin and Nelson¹⁷, (●)Hall and Tompkins¹⁸,
 (—)Tcheurekdjian et al.¹⁹.

IV. THE CRITICAL CLUSTER SIZE

In this section we describe a formalism to evaluate free energy differences between a system containing n molecules and one with $n-1$ molecules at the same temperature and volume. This is then used to estimate the number of water molecules in a cluster of critical size for water adsorbed on the model AgI and on a substrate without surface features that interacts with the water molecules via a Lennard-Jones 9-3 potential. The 9-3 potential depends only on the H_2O -substrate separation distance, z , and results from the Lennard-Jones (6-12) interaction of the given particle with a continuum of atoms in the semi-infinite substrate. The free energy differences are used to estimate the nucleation rate for monolayer formation on these substrates.

In the classical theory of nucleation^{4,6,31}, the (Gibbs) free energy of formation, ΔG , for an embryo of the new phase (at constant temperature and pressure) has a maximum for a value of the radius of the (assumed) spherical droplet. This "critical" radius r^* is obtained by solving the equation $\partial\Delta G/\partial r = 0$. If one considers the system at constant volume V and temperature T , the Helmholtz free energy of formation, ΔF , is maximized at r^* .

In a molecular system at constant V and T , one can define a "critical cluster size" as the number, n^* , of molecules in a cluster whose Helmholtz free energy of formation is a maximum,

and approximate the continuous variable condition $\partial\Delta F/\partial n = 0$ by the discrete equation $\Delta F(n) - \Delta F(n-1) \sim 0^{32}$.

The system to be studied consists of a substrate in the presence of water vapor at a given temperature and vapor pressure. The vapor is formed entirely of water monomers, which adsorb on the substrate forming clusters containing various numbers of molecules. Once formed on the substrate, the adsorbed clusters are assumed to form a mixture of non-interacting ideal gases, i.e., the clusters interact only with the substrate and not with any other cluster. This static model is used to determine an approximate value for the critical cluster size under the given conditions. A steady state model is then assumed in which the clusters grow by diffusion of adsorbed water monomers. This model is used to estimate the steady state nucleation rate J , the number of embryos of the new phase formed per unit area per unit time.

The notation used is as follows:

N_1^O = number of monomers in a vapor at equilibrium with
a surface of liquid water;

N_1^V = number of monomers in the vapor above the substrate;

N_1 = number of monomers adsorbed on the substrate;

N_n = number of adsorbed clusters containing n molecules;

$\Delta F(n)$ = Helmholtz free energy of formation for an n -cluster;

Z_1^V = partition function for a molecule in the vapor;

Z_n = partition function for n molecules on the substrate;
 Q_n = configurational integral for n molecules on the substrate.

The Helmholtz free energy of formation, $\Delta F(n)$, can be defined by

$$N_n = N_1 \exp(-\Delta F(n)/kT) \quad (5)$$

Where N_n is the number of clusters with n molecules. A straightforward statistical mechanical treatment of the system as a mixture of non-interacting ideal gases, (with each collection of n clusters an ideal gas) gives³¹

$$N_n = (N_1/Z_1)^n Z_n. \quad (6)$$

The Z_n is the canonical partition function for n particles:

$$Z_n = B^n Q_n/n! ; \quad B \equiv \Lambda \Lambda_R (8\pi^2 V). \quad (7)$$

Here $\Lambda = (2\pi mkT/h^2)^{3/2}$, $\Lambda_R = \Lambda(I_1 I_2 I_3/4m^3)^{1/2}$, m is the mass of the water molecule, I_i is the i^{th} principal moment of inertia of the rigid molecule, k is Boltzmann's constant, h is Planck's constant, V is the volume and Q_n is the configurational integral²².

We further assume

$$N_1 = N_1^V Z_1 / Z_1^V. \quad (8)$$

From Eqs. (5) and (6), the Helmholtz free energy of formation of the n cluster, $\Delta F(n)$, is given by

$$\Delta F(n)/kT = (1-n) \ln N_1 + n \ln Z_1 - \ln Z_n.$$

Substituting N_1 , Z_1 , and Z_n from Eqs. (7) and (8) we obtain

$$\begin{aligned} \Delta F(n)/kT &= (1-n) \ln N_1^V + \ln Z_1 - \ln Z_n - (1-n) \ln Z_1^V \\ &= (1-n) \ln N_1^V - \ln Q_n + \ln Q_1 + \ln n! \quad (9) \end{aligned}$$

The corresponding Helmholtz free energy of formation for a cluster of $n-1$ molecules is

$$\Delta F(n-1)/kT = (2-n) \ln N_1^V - \ln Q_{n-1} + \ln Q_1 + \ln (n-1)!$$

Therefore

$$\begin{aligned} (\Delta F(n) - \Delta F(n-1))/kT &= -\ln(Q_n/Q_{n-1}) + \ln n - \ln N_1^V \\ &= -\ln(Q_n/Q_{n-1}) - \ln(N_1^O/n) - \ln(N_1^V/N_1^O) \\ &= -C(n) - \ln(N_1^O/n) - \ln S \quad (10) \end{aligned}$$

where we have defined $C(n) \equiv \ln(Q_n/Q_{n-1})$.

The condition that the free energy of formation be a maximum for the critical cluster implies, by Eq. (10), that

$$C(n^*) = \ln(n^*/N_1^0) - \ln S. \quad (11)$$

We evaluate $C(n)$ by a method due to Squire and Hoover³³ as follows. If one writes the total interaction potential energy of the system of n molecules as $U_T = U_0 + \lambda \Delta U$ where ΔU is the interaction potential of one (probe) molecule with the other $n-1$ molecules and U_0 is the interaction potential energy of those $n-1$ molecules, then varying λ from 0 to 1 corresponds to reversibly adding a molecule³³ to the system of $n-1$ molecules.

The configurational integral is then

$$Q_n(\lambda) = (8V\pi^2)^{-n} \int \dots \int \exp(-(U_0 + \lambda \Delta U)/kT) d\mathbf{r}^n,$$

where $d\mathbf{r}^n \equiv \prod d\bar{r}_i \sin\theta_i d\theta_i d\psi_i d\phi_i$, and $d\bar{r}_i$ and $(\psi_i, \theta_i, \phi_i)$ are the differential volume element of the center of mass and Euler angles of the i^{th} (rigid) molecule. Therefore $Q_n(0) = Q_{n-1}$, and from the definition of $C(n)$,

$$C(n) \equiv \ln(Q_n/Q_{n-1}) = \ln(Q_n(1)/Q_n(0))$$

$$\begin{aligned}
&= \ln (Z_n(1)/Z_n(0)) \\
&= - (F_n(1) - F_n(0))/kT.
\end{aligned} \tag{12}$$

The Helmholtz free energy of the n cluster system, as a function of λ is

$$F_n = -kT \ln Z_n = -kTn \ln B - kT \ln Q_n(\lambda). \tag{13}$$

If all the thermodynamic parameters are kept fixed, then

$$\begin{aligned}
dF_n(\lambda) &= (\partial F_n / \partial \lambda) d\lambda = (-kT/Q_n) (\partial Q_n / \partial \lambda) d\lambda \\
&= (-kT/Q_n) (8V\pi^2)^{-n} \cdot \\
&\int (-\Delta U/kT) \exp(-(U_0 + \lambda \Delta U)/kT) dr^n d\lambda \\
&\equiv \langle \Delta U \rangle d\lambda.
\end{aligned} \tag{14}$$

The above expression is the ensemble average of (ΔU) which is calculated with the Metropolis Monte Carlo method.

Integrating λ between 0 and 1, we have

$$(F_n(1) - F_n(0))/(kT) = (1/kT) \int_0^1 \langle \Delta U \rangle d\lambda. \tag{15}$$

Equation (12) then gives

$$C(n) = - (1/kT) \int_0^1 \langle \Delta U \rangle_{MC} d\lambda \tag{16}$$

where $\langle \Delta U \rangle_{MC}$ denotes the Metropolis Monte Carlo average (Appendix C).

It can be shown that for a simple repulsive potential like $V(r) = r^{-9}$, $\langle \Delta U \rangle \rightarrow \lambda^{-2/3}$ as $\lambda \rightarrow 0$. Because of this, Squire and Hoover³³ point out the convenience of modifying this integral and writing it in the form

$$C(n) = (-3/kT) \int_0^1 \lambda^{2/3} \langle \Delta U \rangle d\lambda^{1/3}. \quad (17)$$

We evaluate $C(n)$ for $n = 1, 2, 3, 4, 6$ and 24 water molecules, with the molecules adsorbed on two different substrates, the iodine-exposed basal plane of AgI and a featureless Lennard-Jones substrate. The results are shown in sections A and B.

A. THE SILVER-IODIDE SUBSTRATE

For each cluster size, $n = 1, 2, 3, 4, 6, 24$, the Monte Carlo average of ΔU is calculated for values of λ ranging from 0.05 to 1.0 and plots are made of $-\lambda^{2/3} \langle \Delta U \rangle$ vs. $\lambda^{1/3}$. According to Eq. (17), the value of $C(n)$ is

$$C(n) = (3/kT) (\text{Area under the curve}).$$

An example is shown in Fig. 13 for $n=6$, $T = 265$ °K and the values of $C(n)$ obtained are shown in Fig. 14. The data in Figs. 13 and 14 were obtained by R. Ward and are taken from Ref. 22.

To obtain an estimate for the critical cluster size, we assume a supersaturation ratio $S=1$. With this value of S and the condition $\Delta F(n^*) - \Delta F(n^*-1) = 0$, Eq. (11) implies that the value of n^* is found where the curve for $C(n)$ intersects the curve of $\log(n^*/N_1^0)$. A value of 10.5 is used for the latter (see discussion in section B). Figure 14 indicates an approximate value of $n^* \sim 3$, and a nucleation rate $J \sim 10^{23}$ $\text{cm}^{-2} \text{sec}^{-1}$ is obtained²² by methods described in the next section.

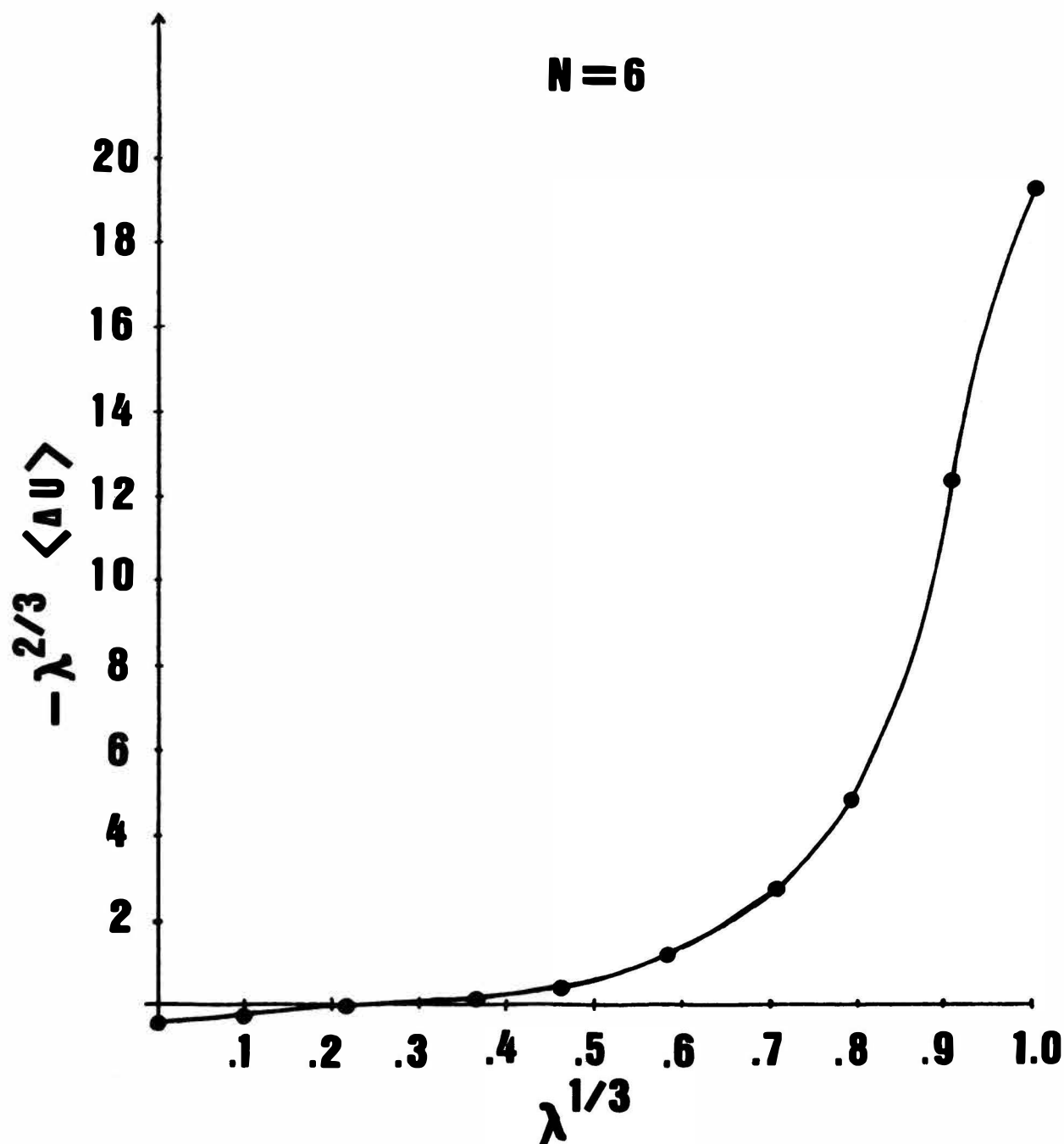


Fig. 13. Plot of $-\lambda^{2/3} \langle \Delta U \rangle$ vs. $\lambda^{1/3}$ for a cluster of $n = 6$ water molecules at 265 °K, adsorbed on the basal plane of silver iodide.²² The value of $C(6)$ is $(3/kT)$ (Area under the curve).

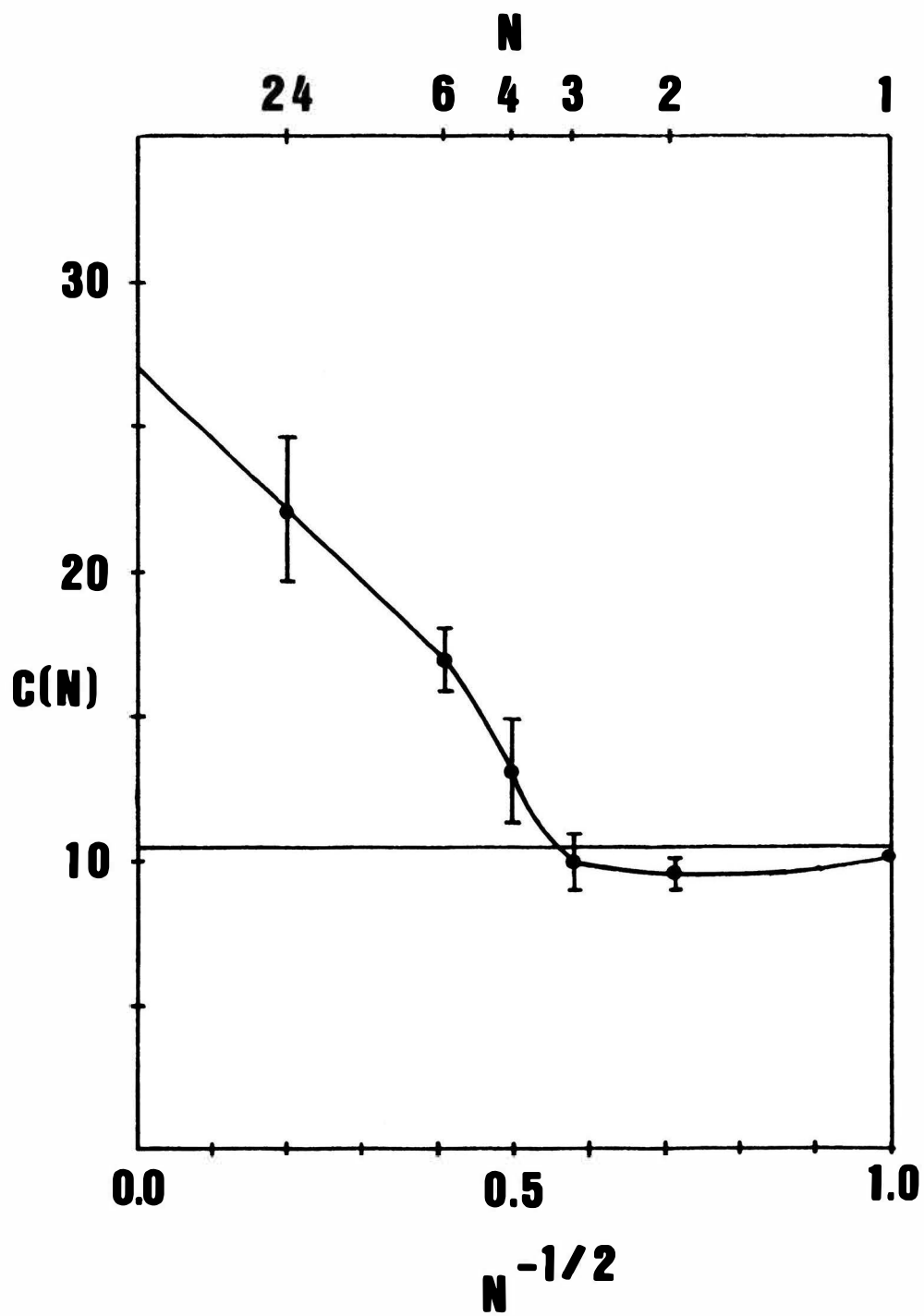


Fig. 14. Plot of $C(n)$ vs. $n^{-1/2}$ for water adsorbed on silver iodide. The intersection of this curve with the horizontal line indicates a critical cluster size of $n^* \sim 3$ molecules for $S = 1$ at 265°K ²².

B. THE SMOOTH LENNARD-JONES SUBSTRATE

In this section we present the calculation of the critical cluster size and the nucleation rate for an ensemble of water molecules adsorbed on a smooth substrate at 265 °K.

1. The model. In this model the water molecules interact with the substrate located in the x-y plane via a 9-3 potential given by:

$$V(z) = V_0 \epsilon (r'^9 - r'^3) ; \text{ where } r' = \sigma/z. \quad (18)$$

Here z is the vertical distance of the water molecule to the x-y plane, and the parameters used are:

$$V_0 = 2.598; \quad \epsilon = 6.5 \text{ kcal/mol}; \text{ and } \sigma = 2.223 \text{ \AA}.$$

These parameters are chosen as follows. The ϵ is taken to be the average H_2O -AgI binding energy per molecule in a large cluster (24 molecules) adsorbed on AgI and the σ is the average H_2O -AgI substrate separation distance. This potential has a minimum value of 6.5 kcal/mol at a distance of $3^{1/6}\sigma$ from the substrate. The 9-3 potential is a continuum approximation to the interaction potential of a particle with a semi-infinite substrate composed of atoms that interact with the given particle via a Lennard-Jones (6-12) potential³⁴.

2. Calculations and results.

a. The critical cluster size. According to Eq. (11), the critical cluster size is given by the intersection of the curve for $C(n)$ with the curve for $\ln(n^*/N_1^0) - \ln S$. We assume $S = 1$, and write $\ln(n^*/N_1^0) = \ln\{(n^*/V)/(N_1^0/V)\}$. The (n^*/V) is determined by the conditions of the Monte Carlo calculations. We use (for all adsorbed cluster sizes) a constant density $n/V = 3.4 \times 10^{21}$ molecules/cm³, corresponding to $\sim 1/10$ of the density in the liquid. We also assume the vapor is at equilibrium with a liquid water surface at 265 °K, giving $N_1^0/V \sim 9.4 \times 10^{16}$ molecules/cm³ where a vapor pressure of 2.5 mm Hg is used to obtain this density³⁵. This gives $\ln(n^*/N_1^0) = \ln\{(n/V)/(N_1^0/V)\} = 10.5$.

The Monte Carlo average of ΔU is calculated for clusters of $n = 1, 2, 3, 4, 6, 24$, and 44 molecules for values of λ from 0.05 to 1.0. A sample of the results is illustrated in Fig. 15 for $n = 6$. According to Eq. (17), the value of $C(6)$ is given by

$$C(6) = (3/kT)(\text{Area under the curve}).$$

This curve gives a value of $C(6) = 16.9 \pm 1$. The uncertainty gives the maximum (minimum) areas under the curve in Fig. 15. The uncertainties in Fig. 15 are estimated from fluctuations of the (cumulative) Monte Carlo average of $\langle \Delta U \rangle$. (See discussion in Appendix C). The same procedure is used to obtain the values of $C(n)$ for all the other clusters. The results are presented in Table IV, and illustrated in Fig. 16. Figure 15 shows a plot of $-\lambda^{2/3} \langle \Delta U \rangle$ vs. $\lambda^{1/3}$. This curve is

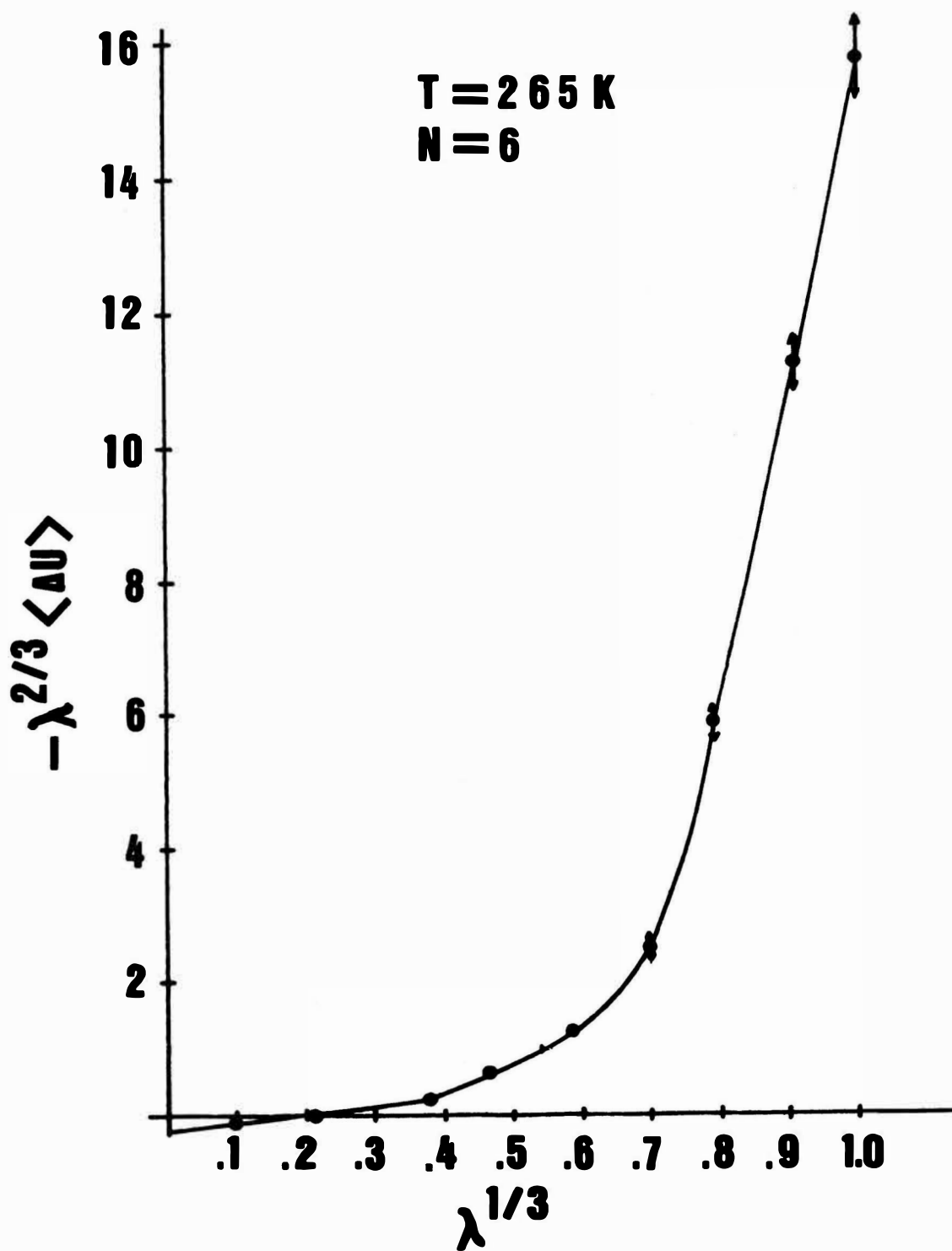


Fig. 15. Plot of $-\lambda^{2/3} \langle \Delta U \rangle$ vs. $\lambda^{1/3}$ for a cluster of $n = 6$ water molecules at $T = 265 \text{ }^\circ\text{K}$ adsorbed on the smooth Lennard-Jones substrate. The value of $C(6)$ is $(3/kT)(\text{Area under the curve})$.

similar to that of silver iodide (Fig. 13) except for a "hump" observed for values of λ close to 1 in the case of AgI. A more detailed analysis is needed to determine if this is a manifestation of the surface structure. Figure 16 shows the plot of $C(n)$ vs. $n^{-1/2}$. $C(n)$ is plotted vs $n^{-1/2}$ for use later in connection with a model for the free energy of formation of adsorbed monolayer clusters. Figure 16 indicates a critical cluster size between 1 and 2 molecules at 265 °K and water saturation.

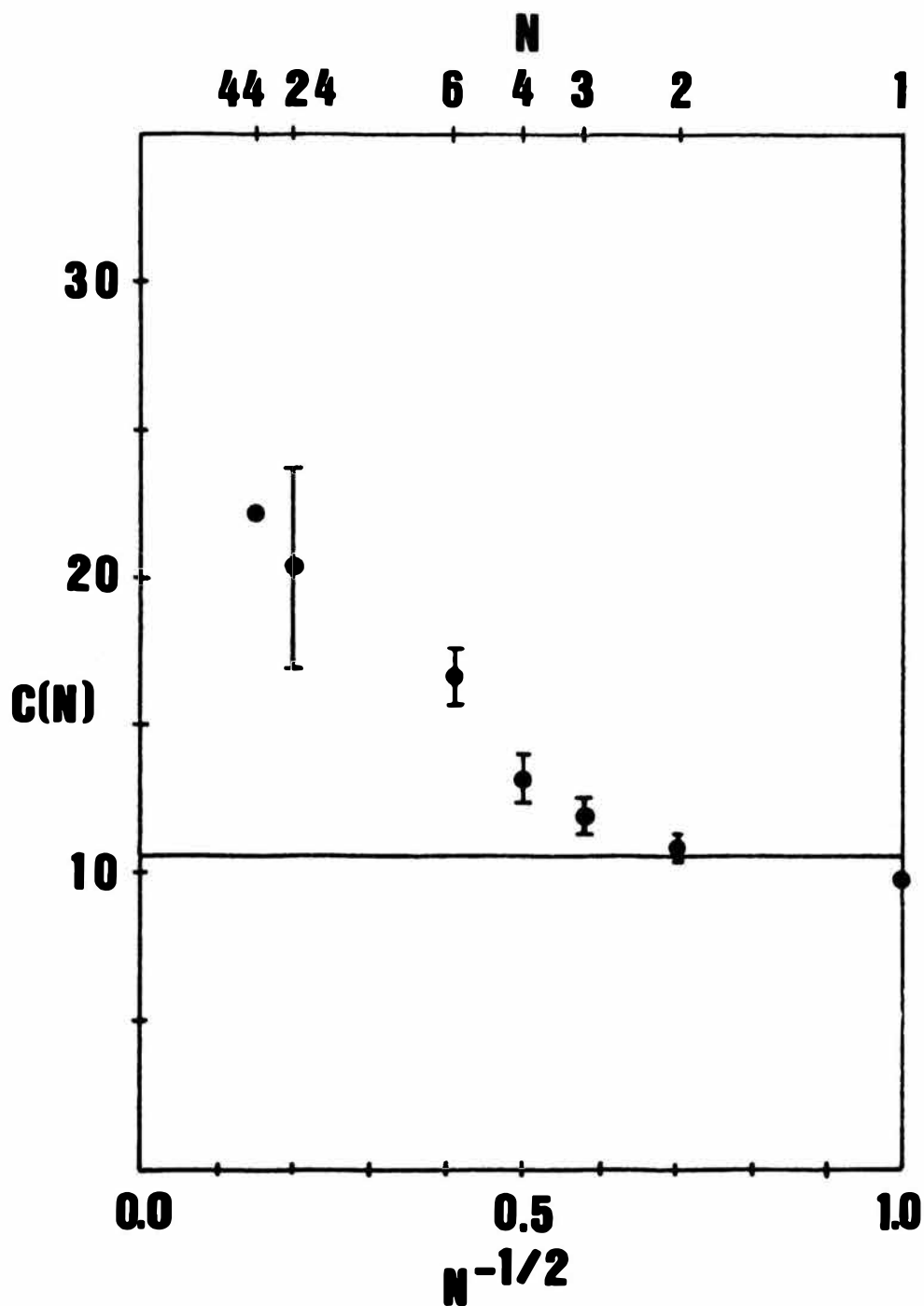


Fig. 16. Plot of $C(n)$ vs. $n^{-1/2}$ for water adsorbed on the smooth Lennard-Jones substrate. The intersection of this curve with the horizontal line indicates a critical cluster size of $n^* \sim 2$ molecules for $S = 1$ at 265°K .

TABLE IV

Calculated values of $C(n)$ for water molecules adsorbed on the smooth Lennard-Jones substrate. The uncertainties reflect the maximum and minimum areas under the curves of $-\lambda^{2/3}\langle\Delta U\rangle$ vs. $\lambda^{1/3}$ (see Fig. 15 for $n=6$). The value of $C(5)$ was estimated from a curve fit and thus no uncertainties are available. The results for $n = 44$ were not run long enough to specify a meaningful uncertainty.

n		C(n)	
1		9.8 ± .1	
2		11.0 ± .5	
3		12.4 ± .8	
4		13.5 ± .9	
5		15.0	
6		16.9 ± 1.0	
24		20.4 ± 3.7	
44		22.	

b. The nucleation rate. In the classical theory of nucleation, the steady state nucleation rate for heterogeneous nucleation is given by³¹

$$J = \left\{ \sum_n (1/\Gamma_n (N_n/A)) \right\}^{-1} \quad (19)$$

where Γ_n is the rate at which monomers attach to a cluster of size n and N_n is the number of such clusters in the area A . The sum ranges over all possible cluster sizes. We calculate N_n as follows²². From Eq.(9), the free energy of formation for a cluster of size n is

$$\Delta F(n)/kT = -\ln Q_n + (1-n) \ln N_1^v + \ln Q_1 + \ln n!.$$

We can rewrite this Eq. as

$$\begin{aligned} \Delta F(n)/kT &= -\ln Q_n + (n-1) \ln (n/N_1^v) + \ln Q_1 + \ln (n!/n^{n-1}) \\ &= -\ln \{ (Q_n/Q_{n-1})(Q_{n-1}/Q_{n-2}) \dots (Q_2/Q_1) \} + \\ &\quad + (n-1) \ln (n/N_1^v) + \ln (n!/n^{n-1}) \\ &= -\sum_{i=2}^n C(i) + (n-1) \ln (n/N_1^v) + \ln (n!/n^{n-1}). \end{aligned} \quad (20)$$

Thus from Eq. (5):

$$N_n = N_1 \exp\{\sum_{i=2}^n C(i) - (n-1) \ln (n/N_1^V) - \ln (n!/n^{n-1})\}. \quad (21)$$

The concentration of monomers on the surface is calculated from Eq. (6):

$$N_1 = N_1^V (Z_1/Z_1^V);$$

thus

$$N_1/A = (N_1^V/N_1^O) (N_1^O/V) (V/A) (Z_1/Z_1^V);$$

and

$$Z_1/Z_1^V = Q_1/Q_1^V = Q_1 = \exp C(1).$$

Where we have defined $C(1) \equiv \ln Q_1$. Therefore

$$N_1/A = S (N_1^O/V) (V/A) \exp C(1).$$

We have $S = 1$, $N_1^O/V = 9.4 \times 10^{16}$ monomers/cm³, $C(1) = 9.8$, and for one molecule $V/A = 2/3 R = 3.5 \times 10^{-8}$ cm (where $R = 5.25$ Å is the radius of the constraining volume for a monomer used in the Monte Carlo calculations) giving $N_1/A \sim 0.57 \times 10^{14}$ monomers/cm². The free energy of formation for a cluster of size n is obtained from Eq. (20) and the corresponding concentration of clusters, N_n , from Eq. (21). The results are given in Table V.

TABLE V

This table shows the free energy of formation (column 6) for a cluster of size n (column 1), calculated from Eq. (20). Columns 2-5 give the quantities that enter into this equation. (Note that the free energy of formation for $n = 24$ and 44 are not given in this table. In order to calculate $\Delta F(n)/kT$ from Eq. (20) all $C(i)$ from $i = 2$ to n must be determined.)

n	$C(n)$	$-\sum C(i)$	$10.5(n-1)$	$\ln(n!/n^{n-1})$	$\Delta F(n)/kT$
2	11.0	-11.0	10.5	0.00	-0.5
3	12.4	-23.4	21.0	-0.41	-2.6
4	13.5	-36.7	31.5	-0.98	-6.2
5	15.0	-51.9	42.0	-1.65	-11.3
6	16.9	-68.8	52.5	-2.38	-18.7

The rate at which monomers strike a cluster of size n , Γ_n , is assumed to be $\Gamma_n = \beta P_n$, where P_n is the perimeter of the n -cluster, $\beta = (N_1/A) \langle v \rangle / 4$ is the number of monomers that cross a unit length per second, and $\langle v \rangle$ is the average speed of a monomer on the surface³¹. For a two dimensional ideal gas $\langle v \rangle = (\pi kT/2m)^{1/2}$. For a water monomer at 265 °K, this gives $\langle v \rangle \sim 4.4 \times 10^4$ cm/sec . Using $N_1/A = 0.57 \times 10^{14}$ monomers/cm², we have $\beta = 0.63 \times 10^{18}$ cm⁻¹ sec⁻¹. The perimeter P_n assumed for each cluster is based on an "effective area" occupied by 24 molecules of 416 Å², giving a radius for this cluster $R \sim 11.5$ Å. The perimeter P_n is then calculated from $P_n = 2\pi r_n = 2\pi R (n/24)^{1/2}$. The perimeter for each cluster and the corresponding value of Γ_n are given below:

$P_1 = 14.8$ Å	$\Gamma_1 = 9.3 \times 10^{10}$ sec ⁻¹
$P_2 = 20.9$ Å	$\Gamma_2 = 1.3 \times 10^{11}$ sec ⁻¹
$P_3 = 25.6$ Å	$\Gamma_3 = 1.6 \times 10^{11}$ sec ⁻¹
$P_4 = 29.5$ Å	$\Gamma_4 = 1.9 \times 10^{11}$ sec ⁻¹
$P_5 = 33.0$ Å	$\Gamma_5 = 2.1 \times 10^{11}$ sec ⁻¹
$P_6 = 36.1$ Å	$\Gamma_6 = 2.3 \times 10^{11}$ sec ⁻¹ .

Substituting these values of Γ_n and the values for N_n/A into Eq. (19), we obtain a nucleation rate

$$J \sim 4 \times 10^{24} \text{ cm}^{-2} \text{ sec}^{-1}.$$

This extremely high value for the nucleation rate indicates that a monolayer forms very rapidly on the substrate at water saturation.

V. CONCLUSION

A. SUMMARY OF RESULTS

The motivation for these studies has been to investigate those features of a substrate which make it a good ice nucleating agent. In particular, we have studied the adsorption of water on two rigid substrates: a model of hexagonal silver iodide and a featureless Lennard-Jones surface. Silver iodide has long been recognized as a good ice nucleant and utilized in cloud seeding. However, only classical (continuum) models for the ice forming process have been used to date. In this work we investigate the adsorption of H_2O on substrates on a microscopic scale using effective pair potentials and Monte Carlo simulation methods. The featureless Lennard-Jones substrate is introduced in this study to distinguish the effects of surface structure on the nucleation of an adsorbed water monolayer.

In the first section we study the interaction of a single water molecule with a model silver iodide substrate containing a chemical defect (a potassium impurity), and a physical defect (a four-layer ledge). The results indicate that both types of imperfections increase the binding energy of the water monomer to the surface, and distort the hexagonal symmetry of preferred adsorption sites exhibited by the defect-free surface. The potassium impurity increases the

binding energy to 23 kcal/mol at the preferred adsorption sites as compared to 16 kcal/mol for the smooth substrate, and these preferred adsorption sites are drawn towards the impurity, perturbing the six fold symmetry observed for the model AgI surface. The four-layer ledge gives a maximum binding energy of 23 kcal/mol, compared to 20 kcal/mol for the prism face and 16 kcal/mol for the favored sites on the iodine exposed basal face of AgI. This increase is due to the larger number of bonds available for the water monomer at the bottom of the ledge.

The above calculations were made assuming an effective charge of 0.6 e for the atoms in the substrate, giving a Boltzmann weighted average for the maximal binding energy over the prism AgI surface of about 20 kcal/mol. This value is considered high when compared to experimental heats of adsorption for low H₂O coverages on AgI. A study of the average binding energy as a function of the charge of the substrate atoms indicates that a more reasonable value for the effective charge in the model potential is 0.4 e, giving an H₂O average binding energy over the (prism AgI) surface of about 11 kcal/mol.

The second part of this study includes the interactions among several adsorbed water molecules. For this study a Metropolis Monte Carlo (MC) method is used to obtain the canonical ensemble averages of thermodynamic properties of water clusters adsorbed on the model silver iodide substrate and on the smooth Lennard-Jones substrate at 265 °K.

A technique due to Squire and Hoover is used to estimate $C(n)$, which is related to the difference in Helmholtz free energies for two systems at the same temperature and volume containing n and $n - 1$ particles, respectively. From this free energy difference we approximate the critical cluster size for nucleation of a water monolayer on the smooth Lennard-Jones substrate. Assuming a supersaturation ratio $S = 1$, we predict a critical cluster size of 1 or 2 molecules at 265 °K, a concentration of monomers on the surface of $\sim 10^{14}/\text{cm}^2$, and a steady state nucleation rate $J \sim 10^{24}$ embryos of the new phase formed per cm^2 per second.

Studies performed by Ward, Hale, and Terrazas²² on the smooth silver iodide substrate (with comparable H_2O -substrate binding and short range forces) indicate a critical cluster size of 3 or 4 molecules and a nucleation rate of $J \sim 10^{23} \text{ cm}^{-2} \text{ sec}^{-1}$ under the same conditions. The smaller critical cluster size and greater nucleation rate for the featureless Lennard-Jones substrate could be a consequence of the absence of preferred adsorption sites. For example, the silver iodide substrate appears to hold the water molecules at specific, preferred adsorption sites, and restrict the orientation of their dipole moment, whereas the smooth substrate allows the H_2O to move and more freely orient their dipole moments. Thus it would appear that the smooth substrate is a better surface for condensation of a water monolayer than the model AgI. However a more complete investigation of the effects of the

long and short range forces (as well as the lattice constants of the model AgI substrate) must be made before a definite conclusion is possible as to the source of the larger nucleation rate on the featureless substrate. The adsorbed clusters on the Lennard-Jones substrate appear to contain more five-membered rings internal to the cluster than the adsorbed clusters on the model AgI. The water clusters on the model AgI substrate contain more six-membered rings and as such are closer in structure to ice I_h . The featureless Lennard-Jones substrate could nucleate an amorphous solid H_2O film at low temperatures. A continuation of this study should include an investigation of temperature effects and the liquid versus solid properties of the adsorbed layer.

B. CONCLUDING REMARKS

The AgI substrates studied here are only models of real systems; and the featureless Lennard-Jones model substrate has no microscopic counterpart in the real world. However, some qualitative conclusions can be drawn from the comparison between results for H_2O monolayer formation on the featureless substrate model and on the structured AgI substrate model. In addition, we feel that the techniques presented in this work can be applied to other model systems with an increasing degree of sophistication. For example, studies are in progress of the critical cluster size and nucleation rate for the adsorption of water on a featureless

Lennard-Jones substrate with an isolated coulombic impurity³⁶. In addition, molecular dynamics calculations are being performed by R.C. Ward for comparison with the Monte Carlo results presented here. In conclusion it is felt that the present studies offer a well defined microscopic approach to the study of H₂O monolayer formation on model substrates. The study can be extended to substrates with a variety of characteristics, whose parameters can be systematically controlled in Monte Carlo (or molecular dynamics) computer experiments.

BIBLIOGRAPHY

1. H.R. Pruppacher and J.D. Klett, Microphysics of Clouds and Precipitation, (D. Reidel, Boston, 1980), Chap. 2.
2. R.R. Rogers, A Short Course in Cloud Physics, (Pergamon Press, New York, 1976), Chap. 11.
3. H.K. Weickmann, "The Development of Bergeron's Ice Crystal Precipitation Theory", Pageoph, 119, 538 (1980/81).
4. B.J. Mason, The Physics of Clouds, (Clarendon Press, Oxford, 1971), Chap. 4.
5. N.H. Fletcher, The Chemical Physics of Ice, (Cambridge U. Press, 1970), Chap. 4.
6. N.H. Fletcher, The Physics of Rainclouds, (Cambridge U. Press, 1969), Chap. 3.
7. B.J. Mason, The Physics of Clouds, (Clarendon Press, Oxford, 1971), Chap. 1.
8. N.H. Fletcher, The Physics of Rainclouds, (Cambridge U. Press, 1969), Chap. 13.
9. Vonnegut, B. , " The nucleation of ice formation by silver iodide", J. Appl. Phys. 18, 593 (1947).
10. B.J. Mason, The Physics of Clouds, (Clarendon Press, Oxford, 1971), p. 222.

11. B.J. Anderson and J. Hallet, *J. Atmos. Sci.*, 33, 822 (1976); G. Gravenhorst and M.L. Corrin, *J. Rech. Atmos.* 6, 205 (1972).
12. B.N. Hale and J. Kiefer, "Studies of Water on AgI Surfaces: An Effective Pair Potential Model", *J. Chem. Phys.* 73, 923 (1980).
13. J. Kiefer and B.N. Hale, "Proceedings of the 9th International Conference on Atmospheric Aerosols, Condensation and Ice Nuclei", Galway, Ireland, 1977, p. 24.
14. J. Kiefer, Ph.D. Dissertation, University of Missouri-Rolla (1979).
15. B.N. Hale, J. Kiefer, S. Terrazas, and R.C. Ward, "Theoretical Studies of Water Adsorbed on Silver Iodide", *J. Phys. Chem.* 84, 1473 (1980).
16. W. Buhrer, R.M. Nicklow, and P. Bruesch, *Phys. Rev. B*, 17, 3362 (1978).
17. M. L. Corrin and J. A. Nelson, *J. Phys. Chem.* 72, 643 (1968).
18. P. G. Hall and F.C. Tompkins, *Trans. Faraday Soc.* 58, 1734 (1962).
19. N. Tcheurekdjian, A.C. Zettlemyer, and J.J. Chessick, *J. Phys. Chem.* 68, 773 (1964).
20. Metropolis, Rosenbluth, Rosenbluth, Teller, and Teller, *J. Chem. Phys.* 21, 1087, (1953).

21. F.H. Stillinger and A. Rahman, J. Chem. Phys., 68, 666 (1978).
22. R. C. Ward, B.N. Hale, and S. Terrazas, "A Study of the Critical Cluster Size for Water Monolayer Clusters on a Model AgI Basal Substrate", J. Chem. Phys. 78, 420 (1983).
23. F.H. Stillinger, Adv. Chem. Phys., 31, 1 (1975).
24. D.M. Adams, Inorganic Solids, Wiley, New York, 1974.
25. Cook, G.A. (ed), Argon, Helium, and the Rare Gases, New York: Interscience (1961), pp. 151 and 317.
26. J.O. Hirschfelder, C.F. Curtiss, and R.B. Bird, "Molecular Theory of Gases and Liquids", Wiley, New York, 1964, p 165.
27. J.O. Hirschfelder, C.F. Curtiss, and R.B. Bird, "Molecular Theory of Gases and Liquids", Wiley, New York, 1964, p 223.
28. J.R. Tessman, A.H. Kahn, and W. Shockley, Phys. Rev., 92, 890 (1953).
29. M.J. Powell, Comput. J., 7, 155 (1964).
30. B.N. Hale, J. Kiefer, and C.A. Ward, J. Chem. Phys. 75, 1991 (1981).
31. F.F. Abraham, Homogeneous Nucleation Theory, Academic Press, New York, 1974, Chap. 1.
32. B. Hale and R.C. Ward, J. Stat. Phys., 28, 487 (1982).

33. D.R. Squire and W.G. Hoover, J. Chem. Phys., 50, 701 (1969).
34. W. Steele, Surf. Sci., 36, 317 (1973).
35. B. Smith, Department of Chemical Engineering, Washington University, St. Louis Missouri, (private communication).
36. S. Terrazas, R. Ward, and B.N. Hale, to be published.
37. J. Kiefer, Ph.D. Dissertation , University of Missouri-Rolla (1979), p 142.
38. K. Binder, Editor, Monte Carlo Methods in Statistical Physics, Springer-Verlag, New York, 1979.
39. J.A. Barker, and R.O. Watts, Chem. Phys. Lett., 3, 144 (1969).

VITA

Sergio Miguel Terrazas was born on May 15, 1952 in Camargo, Chihuahua, Mexico. He received his primary and secondary education in Juarez, Mexico. He received a Bachelor of Science degree in Physics and a Master of Science degree in Physics from the University of Texas at El Paso in December 1975 and August 1977 . He held the Pan American Society Scholarship during his last year of undergraduate work. He has been enrolled in the Graduate School of the University of Missouri-Rolla from August 1977 to December 1981, and from January 1983 to the present. He is a member of Sigma Pi Sigma and Sigma Xi .

APPENDICES

APPENDIX A

THE LENNARD-JONES PARAMETERS FOR THE K-H₂O INTERACTION

For the interaction of polar (p) with non-polar (n) molecules the parameters of the 6-12 Lennard-Jones potential are calculated with the formulas²⁷:

$$\sigma_{pn} = 1/2 (\sigma_p + \sigma_n) \xi^{-1/6}$$

and $\epsilon_{pn} = (\epsilon_p \epsilon_n)^{1/2} \xi^2$.

The $\xi = 1 + \alpha_n \mu^* (\epsilon_p / \epsilon_n)^{1/2} / (4\sigma_n^3)$

and $\mu^* = \mu_p / (\epsilon \sigma_p^3)^{1/2}$ where μ_p = permanent dipole moment.

For water; $\mu_p = 7.058 \text{ (kcal/mol)}^{1/2} \text{ \AA}^{3/2}$

and $\epsilon_w = 4.9 \times 10^{-14} \text{ ergs} = 0.70648 \text{ kcal/mol}$.

This gives $\mu^* = 1.86673$.

The pure-substance parameters used are:

$$\epsilon_I = 3.11 \times 10^{-14} \text{ ergs (Ref. 14);}$$

$$\epsilon_{Ag} = 2.3 \times 10^{-14} \text{ ergs (Ref. 14);}$$

$$\epsilon_K = 1.65 \times 10^{-14} \text{ ergs (Refs. 25,26);}$$

$$\sigma_I = 4.07 \text{ \AA (Ref. 14);}$$

$$\sigma_{Ag} = 3.68 \text{ \AA (Ref. 14);}$$

and $\sigma_K = 3.405 \text{ \AA (Refs. 25,26)}$.

These give:

$$\xi_I = 1.10429,$$

$$\varepsilon_{IW} = 4.76 \times 10^{-14} \text{ ergs} = 0.68635 \text{ kcal/mol},$$

$$\sigma_{IW} = 3.342 \text{ A},$$

$$\xi_{Ag} = 1.06,$$

$$\varepsilon_{AgW} = 0.5467 \text{ kcal/mol},$$

$$\sigma_{AgW} = 3.171 \text{ A},$$

$$\xi_K = 1.05,$$

$$\varepsilon_{KW} = 0.45372 \text{ kcal/mol},$$

and $\sigma_{KW} = 3.04 \text{ A}.$

APPENDIX B

THE INTERACTION POTENTIAL GRID

To circumvent the problem of evaluating the interaction potential of a water molecule with the silver iodide model substrate at every Monte Carlo step, a grid of potential values is created as follows. Within the unit triangle representative of the surface (Fig. 17), the different parts of the potential energy described in Eqs. (3) to (6) are evaluated. The electrostatic potential of a single point charge is calculated using the Ewald summation³⁷. The Lennard-Jones part is also calculated for a point particle (the oxygen), and for the induction part the dipole moment of the water molecule is assumed to point down, perpendicular to the substrate. This procedure is repeated for several unit triangles, with height above the substrate, z , ranging from $z = 0.1 \text{ \AA}$ to $z = 5.0 \text{ \AA}$, in increments of 0.1 \AA . The triangles are then reflected to create the rectangle shown in the lower half of Fig. 18, and this rectangle is itself reflected about the horizontal (dashed) line in Fig. 18 to create the larger rectangle shown. The position of the water molecule anywhere on the substrate can then be translated to a point within the unit cell (the larger rectangle) by subtracting from its x - y coordinates an integer multiple of the dimensions of this unit cell. The total potential for the water molecule is constructed by interpolating between the two adjacent unit

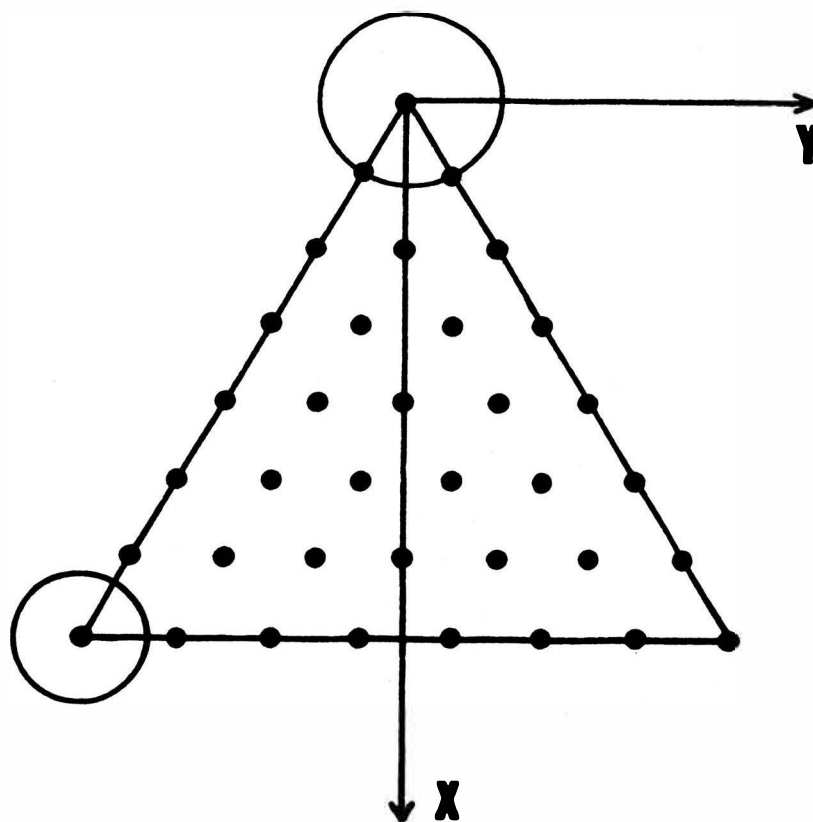


Fig. 17. Points on the triangle representative of the iodine-exposed basal plane of AgI where the interaction of a water molecule with the surface is calculated to create the unit cell shown in Fig. 18.

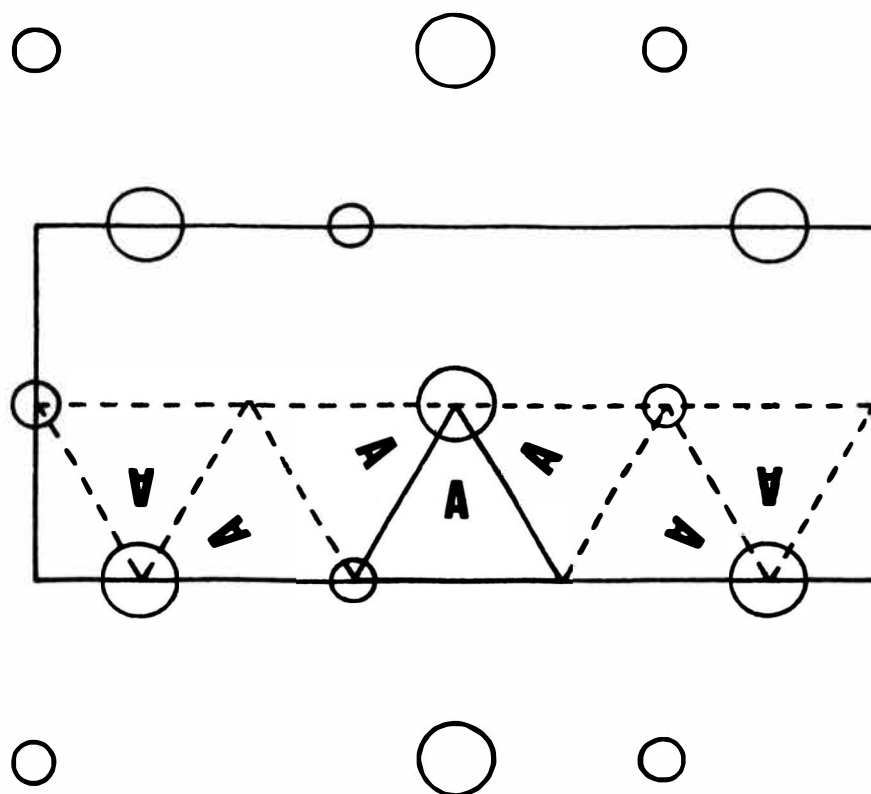


Fig. 18. The unit rectangular cell on the iodine-exposed basal plane of AgI, obtained by reflecting the basic triangle shown at the center of the figure. The orientation of the letter "A" indicates how the reflection is performed. The bottom half of the rectangle is then reflected about the horizontal (dashed) line to obtain the full unit cell.

rectangles for each of the atoms in the water molecule and adding the potential for each atom. The inductive part of the potential, V_{ind} , (which takes into account the orientation of the water dipole moment) is approximated by $V_{ind} = V_0(1 + \cos^2\theta)/2$ where θ is the angle that the dipole moment makes with the negative z axis. The V_0 is the (inductive) energy of the water molecule with its dipole perpendicular to the substrate. While this potential grid only approximates the full potential obtained by summing over all the atoms in the substrate, it provides a feasible evaluation of the H₂O-AgI substrate interaction. This grid is used in all the calculations involving water clusters on AgI.

APPENDIX C

THE MONTE CARLO METHOD

The Monte Carlo method used in this study is due to Metropolis et al.^{20,38}. This method samples the phase space of a model system by comparing the Boltzmann transition probabilities for the system with a random number R , where $0 < R < 1.0$. The Boltzmann probability for a transition from a state i with energy E_i , to a new state j with energy E_j , is given by $P_{ij} = \exp\{- (E_j - E_i)/kT\}$. If $P_{ij} > R$, the new state is accepted and is taken as a new point in the Markov chain. Otherwise the transition is rejected and the old state i is counted again as a new point in the chain. By adding the physical quantity of interest at every point in the chain and dividing by the number of points, one obtains an average that converges to the canonical ensemble average if the chain is long enough. This procedure is illustrated in the flow chart of Fig. 19. The application to (rigid) molecules is the same as that used by Barker and Watts³⁹ and is described in Ref. 22.

The criterion for convergence used in this study is to observe the behavior of the average energy of the system as a function of the number of Monte Carlo steps. The system is considered to have reached equilibrium if the oscillations of the average energy are small (less than 1 kcal/mol). An example is given in Fig. 20 for a system of 6 molecules adsorbed on the smooth Lennard-Jones substrate.

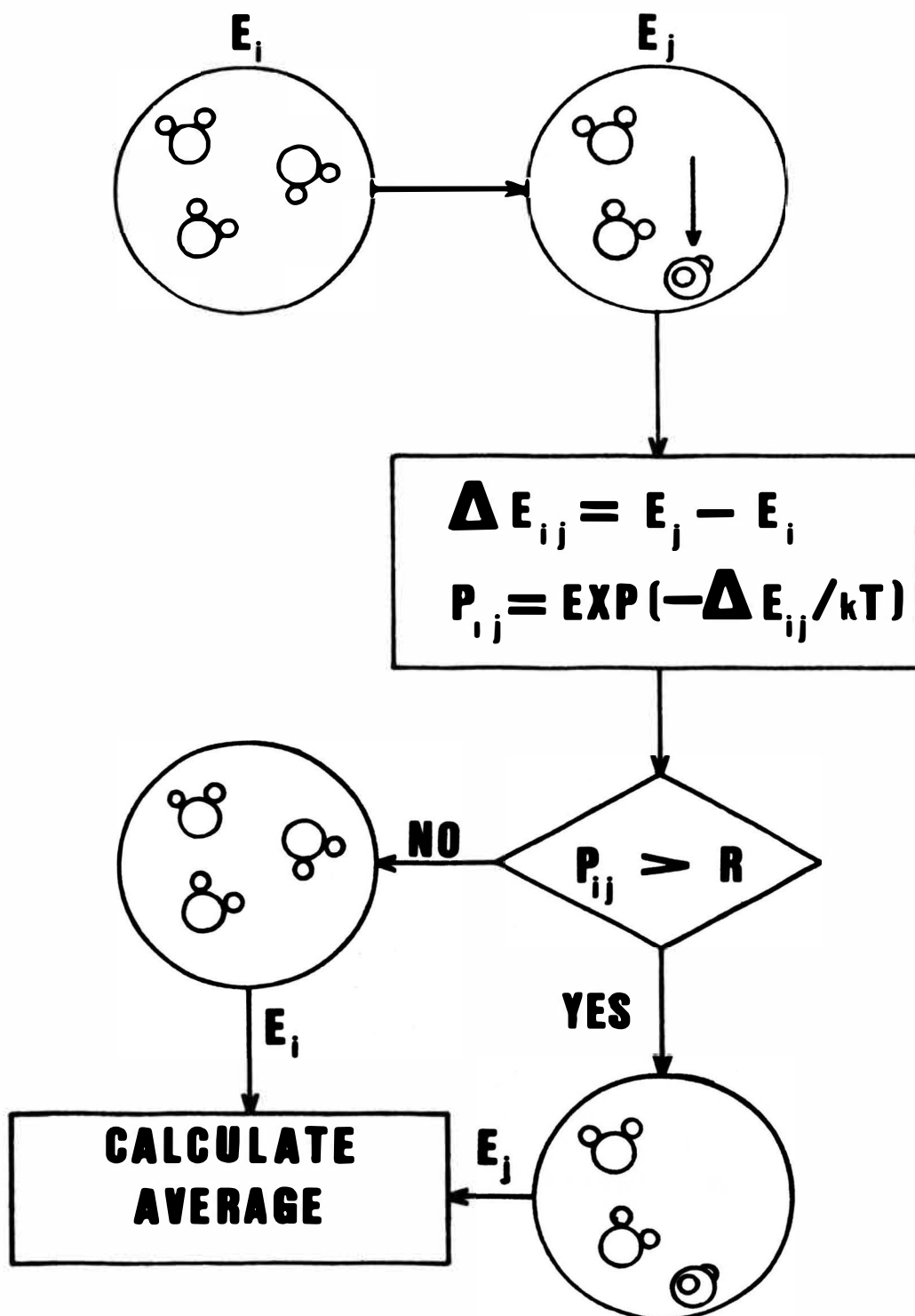


Fig. 19. Flow chart of the Metropolis Monte Carlo method.

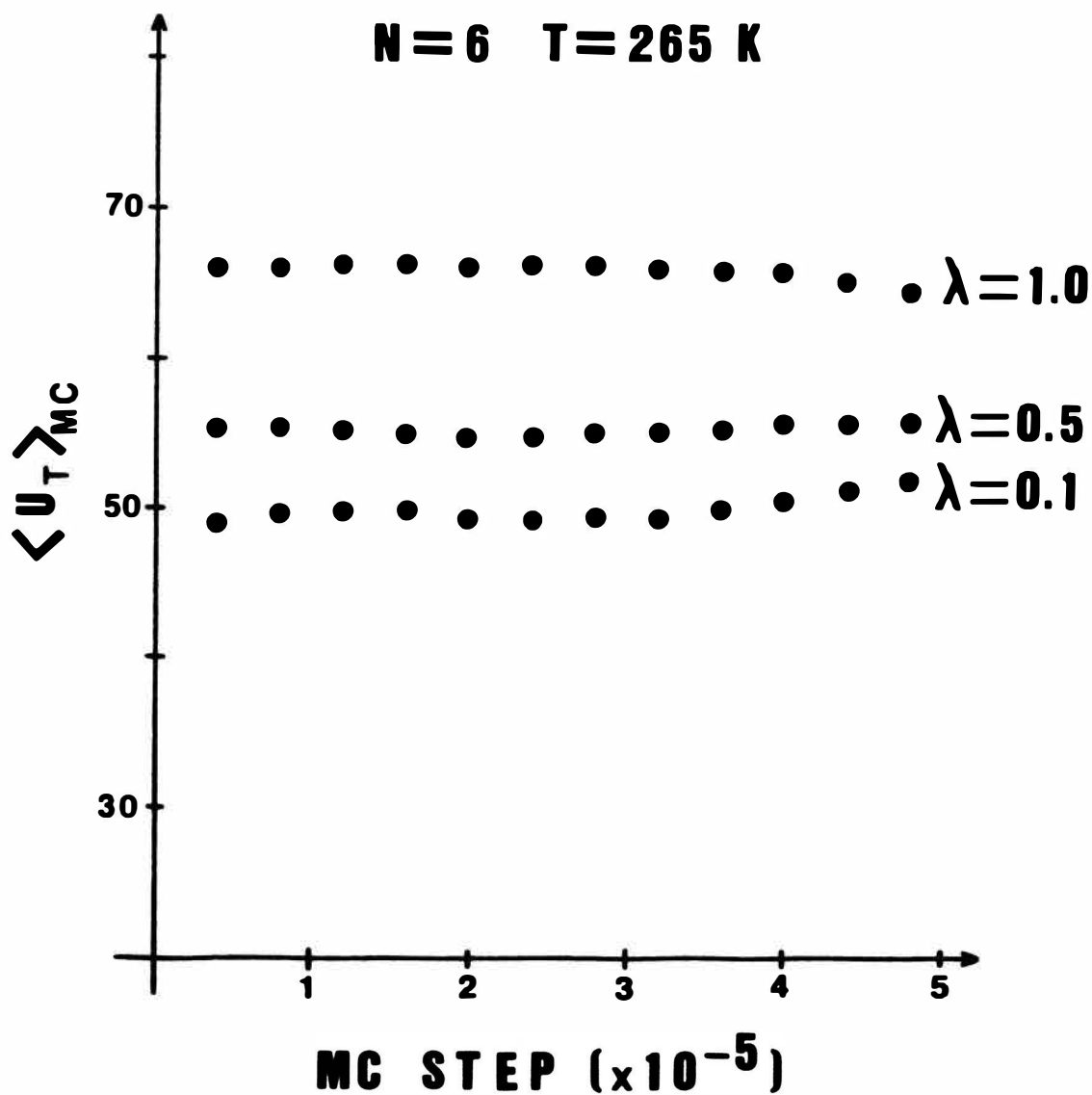


Fig. 20. Average binding energy as a function of the number of Monte Carlo steps for $n = 6$ molecules adsorbed on the smooth Lennard-Jones substrate.

Uncertainties in $\langle \Delta U \rangle$ (referred to on p 45 of the text) arise and are estimated in the present work as follows. The (cumulative) Monte Carlo average of ΔU has fluctuations which, with a sufficient number of Monte Carlo steps, should be negligible. That is, in a "sufficiently long" Monte Carlo run the average of ΔU should be independent of the choice of probe molecule and the length of the run. However, rarely does one have both the man hours and the computer dollars to extend a Monte Carlo run to the "sufficiently long" category. "Sufficiently long" in the Metropolis Monte Carlo method depends on the quantity being averaged. For example the average total potential energy of the system (of say, 6 water adsorbed molecules) usually shows negligible fluctuations (less than 1%) after about 10^6 steps. An average of a quantity such as specific heat for the same system, however, could require as long as $(5-10) \times 10^6$ steps. The ΔU is the interaction potential of the probe molecule with the rest of the system and it is being "turned off" as λ ranges from 1.0 to 0. As λ is decreased the probe molecule can wander away from the cluster ($\Delta U \rightarrow 0$) or, alternatively, can become "too close" to any one of the remaining cluster molecules ($\Delta U \gg 0$). Thus for a large fraction of a short Monte Carlo run the probe molecule can occupy regions of configuration space in which the instantaneous value of ΔU is either close to zero or large and positive without affecting the total potential energy significantly. This qualitative description of the

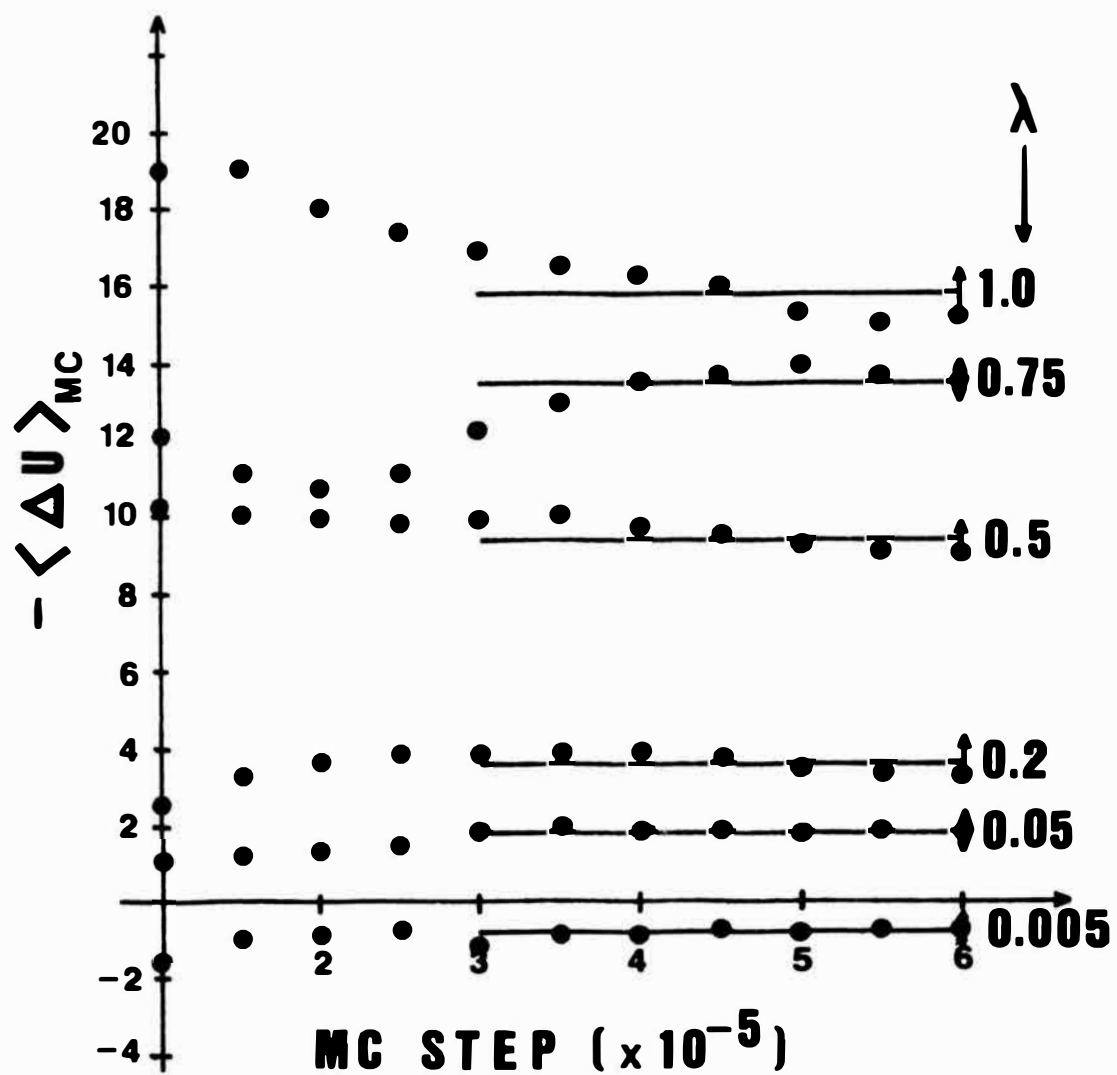


Fig. 21. Average value of ΔU as a function of the number of Monte Carlo steps for $n = 6$ water molecules adsorbed on the smooth Lennard-Jones substrate.

difficulties is reflected in the cumulative averages of ΔU shown in Fig. 21 for six H_2O molecules on the Lennard-Jones substrate. The average values of ΔU used in Fig. 15 for $n = 6$ are assumed to be the lines through the points in Fig. 21, and the uncertainty is estimated from the fluctuations of the cumulative Monte Carlo average of ΔU about these lines. For example for $\lambda = 0.5$ $\Delta U = 9.4 \pm 0.4$. See Fig. 21.